

OVER-PARAMETERIZATION AS A CATALYST FOR BETTER GENERALIZATION OF DEEP RELU NETWORK

Yuandong Tian

Facebook AI Research

yuandong@fb.com

ABSTRACT

To analyze deep ReLU network, we adopt a student-teacher setting in which an over-parameterized student network learns from the output of a fixed teacher network of the same depth, with Stochastic Gradient Descent (SGD). Our contributions are two-fold. First, we prove that when the gradient is zero (or bounded above by a small constant) at every data point in training, a situation called *interpolation setting*, there exists many-to-one *alignment* between student and teacher nodes in the lowest layer under mild conditions. This suggests that generalization in unseen dataset is achievable, even the same condition often leads to zero training error. Second, analysis of noisy recovery and training dynamics in 2-layer network shows that strong teacher nodes (with large fan-out weights) are learned first and subtle teacher nodes are left unlearned until late stage of training. As a result, it could take a long time to converge into these small-gradient critical points. Our analysis shows that over-parameterization plays two roles: (1) it is a necessary condition for alignment to happen at the critical points, and (2) in training dynamics, it helps student nodes cover more teacher nodes with fewer iterations. Both improve generalization. Experiments justify our finding. The code is released in <https://github.com/facebookresearch/luckmatters>.

1 INTRODUCTION

Deep Learning has achieved great success in the recent years (Silver et al., 2016; He et al., 2016; Devlin et al., 2018). Although networks with even one-hidden layer can fit any function (Hornik et al., 1989), it remains an open question how such networks can generalize to new data. Different from what traditional machine learning theory predicts, empirical evidence (Zhang et al., 2017) shows more parameters in neural network lead to better generalization. How over-parameterization yields strong generalization is an important question for understanding how deep learning works.

In this paper, we analyze multi-layer ReLU networks by adopting teacher-student setting. The fixed teacher network provides the output for the student to learn via SGD. The student is over-parameterized (or over-realized): it has more nodes than the teacher. Therefore, there exists student weights whose gradient at *every* data point is zero. Here, we want to study the *inverse* problem:

With small gradient at *every* training sample, can the student weights *recover* the teachers’?

If so, then the generalization performance can be guaranteed if the training converges to such critical points. In this paper, we show that this so-called *interpolation setting* (Ma et al., 2017; Liu & Belkin, 2018; Bassily et al., 2018) leads to *alignment*: under certain conditions, each teacher node is provably aligned with at least one student node in the lowest layer. The condition is simply that the teacher node is *observed* by at least one student node, i.e., teacher’s ReLU boundary lies in the activation region of that student. Therefore, more over-parameterization increases the probability of teachers being observed and thus being aligned. Furthermore, in 2-layer case, those student nodes that are not aligned with any teacher have zero contribution to the output and can be pruned.

Although the interpolation condition gives nice properties, it might not be achievable via training (Ge et al., 2017; Livni et al., 2014). For this, we further analyze the training dynamics and show that most student nodes converge first towards strong teacher nodes with large fan-out weights in magnitude. While this makes training robust to dataset noise and naturally explains implicit regularization, the same mechanism also leaves weak teacher nodes unexplained until very late stage

of training, yielding high generalization error with finite iterations. In this situation, we show that over-parameterization plays another important role: once the strong teacher nodes have been covered, there are always spare student nodes ready to switch to weak teacher nodes quickly. As a result, it enables more teacher nodes to be covered with the same number of iterations, and hence improves generalization after a finite number of training iterations.

One interesting discovery from the analysis is that, the alignment in the lowest layer is very likely to happen even when the top layer weights are random values. Since initialization gives random values of the top layer, it suggests that backpropagation proceeds in a *bottom-up* manner: first the lowest layer moves towards alignment, then second lowest receives good input signals and aligns, etc. In this paper, we only provide with intuitions and leave the formal analysis in the future work.

We justify our findings with numerical experiments on random dataset and CIFAR10.

2 RELATED WORKS

SGD versus GD. Stochastic Gradient Descent (SGD) shows strong empirical performance than Gradient Descent (GD) (Shallue et al., 2018) in training deep models. SGD is often treated as an approximate, or a noisy version of GD (Bertsekas & Tsitsiklis, 2000; Hazan & Kale, 2014; Marceau-Caron & Ollivier, 2017; Goldt et al., 2019; Bottou, 2010). In contrast, many empirical evidences show that SGD achieves better generalization than GD when training neural networks, which is explained via implicit regularization (Zhang et al., 2017; Neyshabur et al., 2015), by converging to flat minima (Hochreiter & Schmidhuber, 1997; Chaudhari et al., 2017; Wu et al., 2018), robust to saddle point (Jin et al., 2017; Daneshmand et al., 2018; Ge et al., 2015; Du et al., 2017) and perform Bayesian inference (Welling & Teh, 2011; Mandt et al., 2017; Chaudhari & Soatto, 2018).

Similar to this work, interpolation setting (Ma et al., 2017; Liu & Belkin, 2018; Bassily et al., 2018) assumes that gradient at each data point vanish at the critical point. While they mainly focus on convergence property of convex objective, we directly relate this condition to specific structure of deep ReLU networks.

Teacher-student/realizable setting. This setting is extensively used in recent works. Due to permutation symmetry, some works start from Tensor decomposition followed by gradient descent (Zhong et al., 2017), others focus on local analysis (e.g., initialization close to the teacher weights or constrained in symmetric cases (Zhong et al., 2017; Tian, 2017; Du et al., 2018)). A line of works (Saad & Solla, 1996; 1995; Goldt et al., 2019; Freeman & Saad, 1997; Mace & Coolen, 1998) studied the dynamics from a statistical mechanics point of view, focusing on local analysis near to some critical points. Usually GD of population/empirical loss of a 2-layer (or one-hidden layer) network is considered, and the input is often assumed to be from Gaussian distribution. Few papers work on teacher-student setting for more than two layers. (Allen-Zhu et al., 2019a) shows the recovery results for 2 and 3 layer networks, with modified SGD and batchsize 1 and heavy over-parameterization.

Local minima is Global. While in deep linear network, all local minima are global (Laurent & Brecht, 2018; Kawaguchi, 2016), situations are quite complicated with nonlinear activations. While local minima is global when the network has invertible activation function and distinct training samples (Nguyen & Hein, 2017; Yun et al., 2018) or Leaky ReLU with linear separate input data (Laurent & von Brecht, 2017), multiple works (Du et al., 2018; Ge et al., 2017; Safran & Shamir, 2017; Yun et al., 2019) show that in GD case with population or empirical loss, spurious local minima can happen even in two-layered network. Many are specific to two-layer and hard to generalize to multi-layer setting. In contrast, our work brings about a generic formulation for deep ReLU network and gives recovery properties in the student-teacher setting.

Over-parameterization. Recent works (Jacot et al., 2018; Du et al., 2019; Allen-Zhu et al., 2019b) show the global convergence of GD for multi-layer networks, when over-parameterization leads to kernel learning. (Li & Liang, 2018; Zou et al., 2018) shows the convergence of in one-hidden layer ReLU network using GD/SGD to solution with good generalization. The input data are assumed to be clustered into classes. The intuition is that over-parameterization leads to “sparse sign changes” of ReLU activations. Both lines of work assume network is heavily over-parameterized: the number of nodes grows polynomially with the number of samples (also in Zou & Gu (2019)) or grows polynomially with the population loss (Cao & Gu, 2019).

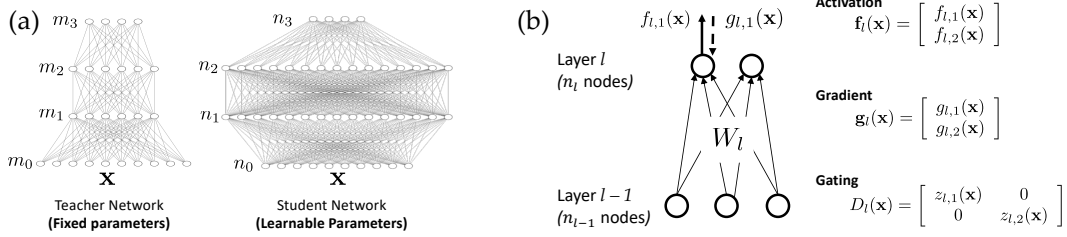


Figure 1: Problem Setup. **(a)** Student-teacher setting. The student network learns from the output of a fixed teacher network via stochastic gradient descent (SGD). **(b)** Notations. All low cases are scalar, bold lower case are column vectors (row vectors are always with a transpose) and upper cases are matrices.

Combined with student-teacher setting, (Goldt et al., 2019) assumes Gaussian input and symmetric parameterization to analyze local structure around critical points, (Tian et al., 2019) gives convergence results for 2-layer network when a subset of the student network is close to the teacher. These cases assume mild over-parameterization but only achieve local results. Other works show global convergence of over-parameterized network but with optimal transport (Chizat & Bach, 2018) which is only practical with low-dimensional input. Our work extends (Tian et al., 2019) with much fewer and weaker assumptions, provides analysis on critical point and training dynamics.

3 MATHEMATICAL FRAMEWORK

Using Teacher Network. The reason why we formulate the problem using teacher network rather than a dataset is the following: **(1)** It leads to a nice and symmetric formulation for multi-layered ReLU networks (Lemma 1). **(2)** A teacher network corresponds to a dataset of infinite size. This separates the finite sample issues from inductive bias in the dataset. This also separates issues due to inductive bias from issues due to optimization. **(3)** A generalization bound for arbitrary function class can be hard. With teacher network, we implicitly enforce an inductive bias corresponds to the structure of teacher network, which could lead to better generalization bound. **(4)** If student weights can be shown to converge to teacher ones, generalization naturally follows for the student.

Notation. Consider a student network and its associated teacher network (Fig. 1(a)). Denote the input as \mathbf{x} . We focus on multi-layered networks with the activation function $\sigma(\cdot)$ as the ReLU non-linearity. We use the following equality extensively: $\sigma(x) = \mathbb{I}[x > 0]x$, where $\mathbb{I}[\cdot]$ is the indicator function. For node j , $f_j(\mathbf{x})$, $z_j(\mathbf{x})$ and $g_j(\mathbf{x})$ are its activation, gating function and backpropagated gradient *after the gating*.

Both teacher and student networks have L layers. The input layer is layer 0 and the topmost layer (layer that is closest to the output) is layer L . For layer l , let m_l be the number of teacher nodes while n_l be the number of student nodes. $W_l \in \mathbb{R}^{n_{l-1} \times n_l}$ is the weight matrix connecting layer $l-1$ to layer l on the student side. $W_l = [\mathbf{w}_{l,1}, \mathbf{w}_{l,2}, \dots, \mathbf{w}_{l,n_l}]$ where each $\mathbf{w} \in \mathbb{R}^{n_{l-1}}$ is the weight vector. Similarly we have teacher weight $W_l^* \in \mathbb{R}^{m_{l-1} \times m_l}$. Finally, $\mathcal{W} = \{W_1, W_2, \dots, W_L\}$ as the collection of all trainable parameters.

Let $\mathbf{f}_l(\mathbf{x}) = [f_{l,1}(\mathbf{x}), \dots, f_{l,n_l}(\mathbf{x})]^\top \in \mathbb{R}^{n_l}$ be the activation vector of layer l , $D_l(\mathbf{x}) = \text{diag}[z_{l,1}(\mathbf{x}), \dots, z_{l,n_l}(\mathbf{x})] \in \mathbb{R}^{n_l \times n_l}$ be the diagonal matrix of gating function. For ReLU, the diagonal element is either 0 or 1. Let $\mathbf{g}_l(\mathbf{x}) = [g_{l,1}(\mathbf{x}), \dots, g_{l,n_l}(\mathbf{x})]^\top \in \mathbb{R}^{n_l}$ be the backpropagated gradient vector. By definition, the input layer has $\mathbf{f}_0(\mathbf{x}) = \mathbf{x} \in \mathbb{R}^{n_0}$ and $m_0 = n_0 = d$, where d is the input dimension. Note that $\mathbf{f}_l(\mathbf{x})$, $\mathbf{g}_l(\mathbf{x})$ and $D_l(\mathbf{x})$ are all dependent on \mathcal{W} . For notation brevity, we often use $\mathbf{f}_l(\mathbf{x})$ rather than $\mathbf{f}_l(\mathbf{x}; \mathcal{W})$.

All notations with superscript $*$ are only dependent on the teacher and remains constant throughout the training. At the output (topmost) layer, $D_L^*(\mathbf{x}) = D_L(\mathbf{x}) \equiv I_{C \times C}$ since there is no ReLU gating. Note that $C = m_L = n_L$ is the dimension of output for both teacher and student. With the notation, gradient flow update can be written as:

$$\dot{W}_l = \mathbb{E}_{\mathbf{x}} [\mathbf{f}_{l-1}(\mathbf{x}) \mathbf{g}_l^\top(\mathbf{x})] \quad (1)$$

In SGD, the expectation $\mathbb{E}_{\mathbf{x}}[\cdot]$ is taken over a batch. In GD, it is over the entire dataset.

Bias term. Note that with the same notation we can also include the bias term. In this case, $W_l \in \mathbb{R}^{(n_{l-1}+1) \times n_l}$, $\mathbf{w}_{l,1} = [\tilde{\mathbf{w}}_{l,1}^\top, b_{l,1}]^\top \in \mathbb{R}^{n_{l-1}+1}$, $\mathbf{f}_l = [\hat{\mathbf{f}}_l^\top, 1]^\top \in \mathbb{R}^{n_l+1}$, $\mathbf{g}_l \in \mathbb{R}^{n_l+1}$ and $D_l \in \mathbb{R}^{(n_l+1) \times (n_l+1)}$ (last diagonal element is always 1). In the text, by slightly abuse of notation, we will not distinguish the cases with bias or without bias.

Objective. We assume that both the teacher output $\mathbf{f}_L^*(\mathbf{x})$ and the student output $\mathbf{f}_L(\mathbf{x})$ are vectors of length C . We use the output of teacher as the input of the student and the objective is:

$$\min_{\mathcal{W}} J(\mathcal{W}) = \frac{1}{2} \mathbb{E}_{\mathbf{x}} [\|\mathbf{f}_L^*(\mathbf{x}) - \mathbf{f}_L(\mathbf{x})\|^2] \quad (2)$$

By the backpropagation rule, we know that for each sample \mathbf{x} , the (negative) gradient $\mathbf{g}_L(\mathbf{x}) \equiv \partial J / \partial \mathbf{f}_L = \mathbf{f}_L^*(\mathbf{x}) - \mathbf{f}_L(\mathbf{x})$. The gradient gets backpropagated until the first layer is reached.

Note that here, the gradient $\mathbf{g}_L(\mathbf{x})$ sent to layer L is *correlated* with the activations $\mathbf{f}_L^*(\mathbf{x})$ and $\mathbf{f}_L(\mathbf{x})$ at the same layer. Intuitively, this means that the gradient “pushes” the student node j to align with output dimension j of the teacher. A natural question arises:

Are student nodes correlated with teacher nodes at the same layers after training? (*)

One might wonder this is hard since the student’s intermediate layer receives no *direct supervision* from the corresponding teacher layer, but relies only on backpropagated gradient. Surprisingly, the following theorem shows that it is possible to build connections at the intermediate layers:

Lemma 1 (Recursive Gradient Rule). *At layer l , the backpropagated $\mathbf{g}_l(\mathbf{x})$ satisfies*

$$\mathbf{g}_l(\mathbf{x}) = D_l(\mathbf{x}) [A_l(\mathbf{x}) \mathbf{f}_l^*(\mathbf{x}) - B_l(\mathbf{x}) \mathbf{f}_l(\mathbf{x})], \quad (3)$$

where the mixture coefficient $A_l(\mathbf{x}) = V_l^\top(\mathbf{x}) V_l^*(\mathbf{x}) \in \mathbb{R}^{n_l \times m_l}$ and $B_l(\mathbf{x}) = V_l^\top(\mathbf{x}) V_l(\mathbf{x}) \in \mathbb{R}^{n_l \times n_l}$. The matrices $V_l(\mathbf{x}) \in \mathbb{R}^{C \times n_l}$ and $V_l^*(\mathbf{x}) \in \mathbb{R}^{C \times m_l}$ are defined in a top-down manner:

$$V_{l-1}(\mathbf{x}) = V_l(\mathbf{x}) D_l(\mathbf{x}) W_l^\top, \quad V_{l-1}^*(\mathbf{x}) = V_l^*(\mathbf{x}) D_l^*(\mathbf{x}) W_l^{*\top} \quad (4)$$

In particular, $V_L(\mathbf{x}) = V_L^*(\mathbf{x}) = I_{C \times C}$.

For convenience, we can write $V_l(\mathbf{x}) = [\mathbf{v}_{l,1}(\mathbf{x}), \mathbf{v}_{l,2}(\mathbf{x}), \dots, \mathbf{v}_{l,n_l}(\mathbf{x})]$ in which $\mathbf{v}_{l,j}(\mathbf{x}) \in \mathbb{R}^C$. Each element of A_l , $\alpha_{l,jj'}(\mathbf{x}) = \mathbf{v}_{l,j}^\top(\mathbf{x}) \mathbf{v}_{l,j'}^*(\mathbf{x})$ and each element of B_l , $\beta_{l,jj'}(\mathbf{x}) = \mathbf{v}_{l,j}^\top(\mathbf{x}) \mathbf{v}_{l,j'}(\mathbf{x})$. Note that Lemma 1 applies to arbitrarily deep ReLU networks and allows different number of nodes for the teacher and student. In particular, student can be over-parameterized (or over-realized).

Let $R_0 = \{\mathbf{x} : \rho(\mathbf{x}) > 0\} \subset \mathbb{R}^d$ be the *infinite* training set, where $\rho(\mathbf{x})$ is the input data distribution. Unlike previous works, we don’t impose any distributional assumption on $\rho(\cdot)$. Let $R_l = \{\mathbf{f}_l(\mathbf{x}) : \mathbf{x} \in R_0\} \subset \mathbb{R}^{n_d}$, which is the image of the training set at the output of layer l . Then the mixture coefficient $A_l(\mathbf{x})$ and $B_l(\mathbf{x})$ have the following property:

Corollary 1 (Piecewise constant). *R_0 can be decomposed into a finite (but potentially exponential) set of regions $\mathcal{R}_{l-1} = \{R_{l-1}^1, R_{l-1}^2, \dots, R_{l-1}^J\}$ plus a zero-measure set, so that $A_l(\mathbf{x})$ and $B_l(\mathbf{x})$ are constant within each region R_{l-1}^j with respect to \mathbf{x} .*

4 CRITICAL POINT ANALYSIS

It seems hard to achieve the goal (*) since the student intermediate node doesn’t have direct supervision from the teacher intermediate node, and there exists many different ways to explain teacher’s supervision. However, thanks to the property of ReLU node and subset sampling in SGD, at SGD critical point, under mild condition, the teacher node aligns with at least one student node.

4.1 SGD CRITICAL POINTS LEADS TO INTERPOLATION SETTING

Definition 1 (SGD critical point). *$\hat{\mathcal{W}}$ is a SGD critical point if for any batch, $\dot{W}_l = 0$ for $1 \leq l \leq L$.*

Theorem 1 (Interpolation). *Denote $\mathcal{D} = \{\mathbf{x}_i\}$ as a dataset of N samples. If $\hat{\mathcal{W}}$ is a critical point for SGD, then either $\mathbf{g}_l(\mathbf{x}_i; \hat{\mathcal{W}}) = \mathbf{0}$ or $\mathbf{f}_{l-1}(\mathbf{x}_i; \hat{\mathcal{W}}) = \mathbf{0}$.*

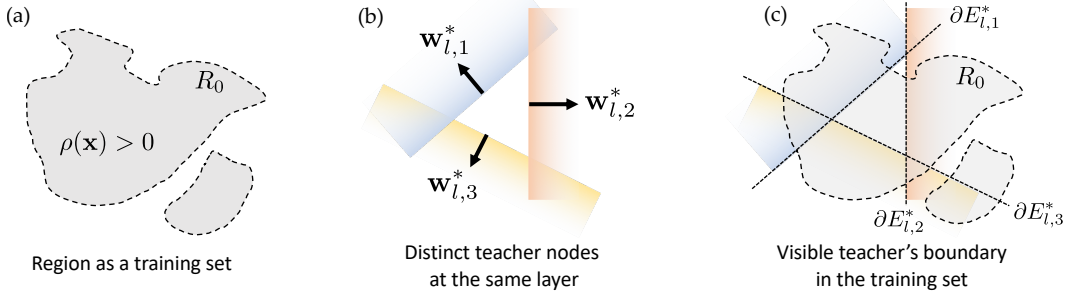


Figure 2: Basic assumptions for Theorem 2 and 4: (a) Training set is a region R_0 in the input space, can be nonconvex or even not-connected, (b) For layer $l = 1$, teacher nodes of the same layer are distinct ($\mathbf{w}_{l,j}^* \neq \mathbf{w}_{l,j'}$ for $j \neq j'$), (c) All teacher boundaries are *visible* in the training set. Here $\partial E_{l,j}^* \cap R_0 \neq \emptyset$ for $j = 1, 2, 3$.

Note that such critical points exist since student is over-parameterized. In this case, critical points in SGD is much stronger than those in GD, where the gradient is always averaged at a fixed data distribution. Note that if \mathbf{f}_{l-1} has bias term, then $\mathbf{f}_{l-1} \neq \mathbf{0}$ always and $\mathbf{g}_l(\mathbf{x}_i; \hat{\mathcal{W}}) = \mathbf{0}$. For topmost layer, immediately we have $\mathbf{g}_L(\mathbf{x}_i; \hat{\mathcal{W}}) = \mathbf{f}_L^*(\mathbf{x}_i) - \mathbf{f}_L(\mathbf{x}_i) = \mathbf{0}$, which is global optimum with zero training loss. In the following, we want to check whether this condition leads to generalization, i.e., whether the teacher's weights are *recovered* or *aligned* by the student, i.e., whether for teacher j , there exists a student k at the same layer so that $\mathbf{w}_k = \gamma \mathbf{w}_j$ for some $\gamma > 0$ (bias term included).

4.2 ASSUMPTION OF TEACHER NETWORK

Obviously, not all teacher networks can be properly reconstructed. A trivial example is that a teacher network always output zero since all the training samples lie in the inactive halfspace of its ReLU nodes. Therefore, we need to impose condition on the teacher network.

Let $E_j = \{\mathbf{x} : f_j(\mathbf{x}) > 0\}$ be the activation region of node j . Note that the halfspace E_j is an open set. Let $\partial E_j = \{\mathbf{x} : f_j(\mathbf{x}) = 0\}$ be the decision boundary of node j .

Definition 2 (Observer). *Node k is an observer of node j if $E_k \cap \partial E_j \neq \emptyset$. See Fig. 4(a).*

Definition 3 (Alignment/Co-linearity). *Node k aligns with node j , if $\mathbf{w}_k = \gamma \mathbf{w}_j$ with some $\gamma > 0$.*

Without loss of generality, we set all teacher nodes to be normalized: $\|\mathbf{w}_{l,j}^*\|_2 = 1$ (bias included in l^2 -norm), except for the topmost layer $l = L$. For the teacher node at layer l , we impose additional condition:

Assumption 1 (Teacher Network Condition at layer l). *We require that (1) the teacher weights $\mathbf{w}_{l,j}^*$ are not co-linear. and (2) the boundary of $\mathbf{w}_{l,j}^*$ is visible in the training set: $\partial E_{l,j}^* \cap R_{l-1} \neq \emptyset$.*

Fig. 2 visualizes the two assumptions. The first requirement is trivial to satisfy. For the second requirement, since two teacher nodes (or two consecutive layers) who behaves linearly in the training set are indistinguishable, if we want to reconstruct weight W_l , we would need the second requirement to hold at layer l . If not, then one counter-example is that there exist identity mappings from layer $l - 1$ to layer l , and non-identity mapping (real operations) from layer l to layer $l + 1$. In this case, there is ambiguity whether these real operations are performed in W_l or W_{l+1} and reconstruction will not follow.

In the following, we remove the subscript l when $l = 1$ for notation brevity.

4.3 ALIGNMENT OF TEACHER WITH STUDENT, 2-LAYER CASE

We start with 2-layer case, in which $A_1(\mathbf{x})$ and $B_1(\mathbf{x})$ are constant over \mathbf{x} , since there is no ReLU gating at the top layer $l = L = 2$. In this case, from the SGD critical point at $l = 1$, $\mathbf{g}_1(\mathbf{x}) = D_1(\mathbf{x}) [A_1 \mathbf{f}_1^*(\mathbf{x}) - B_1 \mathbf{f}_1(\mathbf{x})] = \mathbf{0}$ and alignment between teacher and student can be achieved:

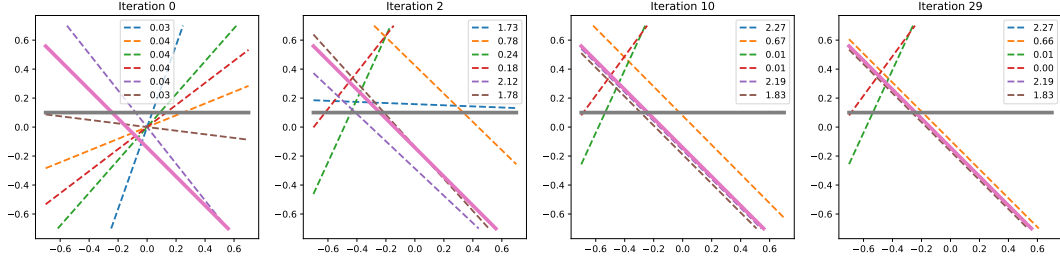


Figure 3: Convergence (2 dimension) for 2 teachers (solid line) and 6 students (dashed line). Legend shows $\|\mathbf{v}_k\|$ for student node k . $\|\mathbf{v}_k\| \rightarrow 0$ for nodes that are not aligned with teacher.

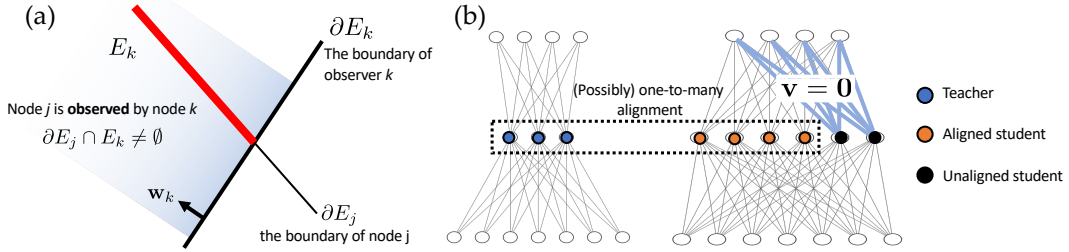


Figure 4: (a) The definition of *observer* (See Def. 2). (b) Alignment patterns. A teacher can be aligned with multiple students. Students who are not aligned with either teacher or other students will have zero fan-out weights, if they are observed by sufficient number of student nodes (Theorem 3).

Theorem 2 (Student-teacher Alignment, 2-layers). *If Assumption 1 holds for $l = 1$, at SGD critical point, if a teacher node j is observed by a student node k and $\alpha_{k,j} \neq 0$, then there exists at least one student node k' aligned with j .*

Proof sketch. The intuition is that ReLU activations $\sigma(\mathbf{w}_k^\top \mathbf{x})$ can be proven to be mutually linear independent, if their boundaries are within the training region R_0 . For details, please check Lemma 2, Lemma 3 and Lemma 6 in the Appendix. On the other hand, the gradient of each student node k when active, is $\alpha_k^\top \mathbf{f}_1(\mathbf{x}) - \beta_k^\top \mathbf{f}_1(\mathbf{x}) = 0$, a linear combination of teacher and student nodes (note that α_k^\top and β_k^\top are k -th rows of A_1 and B_1). Therefore, zero gradient means that the summation of coefficients of co-linear ReLU nodes is zero. Since teachers are not co-linear (Assumption 1), a non-zero coefficient $\alpha_{k,j} \neq 0$ for teacher j means that it has to be co-linear with at least one student node, so that the summation of coefficients is zero. Alignment with multiple student nodes is also possible. In contrast, for deep linear models, alignment does not happen since a linear subspace spanned by intermediate layer can be represented by different sets of bases.

Note that a necessary condition of a reconstructed teacher node is that its boundary is in the active region of student, or is *observed* (Definition 2). This is intuitive since a teacher node which behaves like a linear node is partly indistinguishable from a bias term.

For student nodes that are not aligned with the teacher, if they are observed by other student nodes, then following a similar logic, we have the following:

Theorem 3 (Unaligned Student Nodes are Prunable). *If Assumption 1 holds for $l = 1$, at SGD critical point, if an unaligned student k has C independent observers, i.e., the C -by- C matrix stacking the fan-out weights \mathbf{v} of these observers is full rank, then $\sum_{k' \in \text{co-linear}(k)} \mathbf{v}_{k'} \|\mathbf{w}_{k'}\| = \mathbf{0}$. In particular, if node k is not co-linear with any other student, then $\mathbf{v}_k = \mathbf{0}$.*

Corollary 2. *With sufficient observers, the contribution of all unaligned student nodes is zero.*

The alignment patterns are summarized in Fig. 4(b). Theorem 3 and Corollary 2 explain why network pruning is possible (LeCun et al., 1990; Hassibi et al., 1993; Hu et al., 2016). With these alignment patterns, we could also explain why low-cost critical points can be connected via line segments, but not a single straight line, like what (Kuditipudi et al., 2019) explains, but without as-

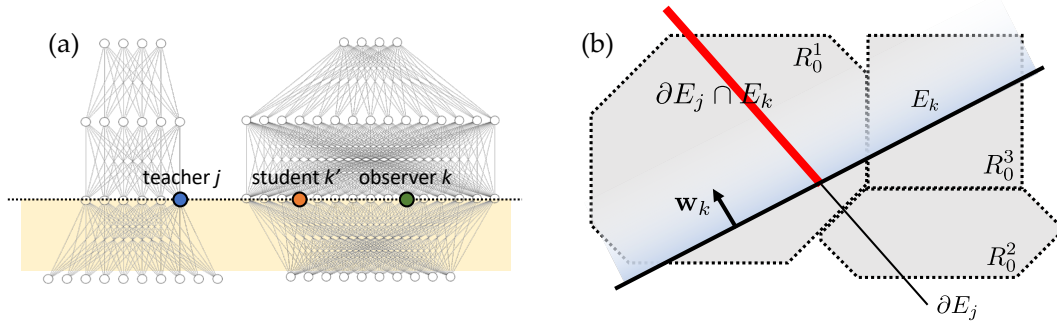


Figure 5: (a) In the multiple layer case, the same proof logic can be applied to the lowest layer (yellow region), because (b) $A_l(\mathbf{x})$ and $B_l(\mathbf{x})$ are now constant in regions R_0^1, R_0^2 , etc. We omit subscript l for brevity.

suming their condition of ϵ -dropout stableness of a trained network. In fact, according to the analysis above, it already holds at SGD critical points.

Our theorem is also consistent with Theorem 5 in (Tian et al., 2019) which also shows the fan-out weights are zero up on convergence in 2-layer networks, if the initialization is close. In contrast, Theorem 3 analyzes the critical point rather than the local dynamics near the critical points.

Note that a related theorem (Theorem 6) in (Laurent & von Brecht, 2017) studies 2-layer network with scalar output and linear separable input, and discusses characteristics of individual data point contributing loss in a local minima of GD. In our paper, no linear separable condition is imposed.

4.4 MULTI-LAYER CASE

Thanks to Lemma 1 which holds for deep ReLU networks, we can use similar intuition as in the 2-layer case, to analyze the behavior of the lowest layer ($l = 1$) in the multiple layer case. The difference here is that $A_1(\mathbf{x})$ and $B_1(\mathbf{x})$ are no longer constant over \mathbf{x} . Fortunately, using Corollary 1, we know that $A_1(\mathbf{x})$ and $B_1(\mathbf{x})$ are piece-wise constant that separate the input region R_0 into a finite (but potentially exponential) set of constant regions $\mathcal{R}_0 = \{R_0^1, R_0^2, \dots, R_0^J\}$ plus a zero-measure set. This suggests that we could check each region separately. If the boundary of a teacher j and a student k lies in the region (Fig. 5), similar logic applies:

Theorem 4 (Student-teacher Alignment, Multiple Layers). *If Assumption 1 holds for $l = 1$, at SGD critical points, for any teacher node j at $l = 1$, if there exists a region $R \in \mathcal{R}$ and a student observer k so that $\partial E_j^* \cap E_k \cap R \neq \emptyset$ and $\alpha_{kj}(R) \neq 0$, then node j aligns with at least one student node k' .*

The theorem suggests a few interesting consequences:

The role of over-parameterization. Theorem 2 and Theorem 4 suggest that over-parameterization (more student nodes in the hidden layer $l = 1$) is important. More student nodes mean more observers, and the existence argument in these theorems is more likely to happen and more teacher nodes can be covered by student, yielding better generalization.

Bottom-up training. Note that even with random $V_1(\mathbf{x})$ (e.g., at initialization), Theorem 4 still holds with high probability (when $\alpha_{kj} \neq 0$) and teacher $\mathbf{f}_1^*(\mathbf{x})$ can still align with student $\mathbf{f}_1(\mathbf{x})$. This suggests a picture of *bottom-up training* in backpropagation: After the alignment of activations at layer 1, we just treat layer 1 as the low-level features and the procedure repeats until the student matches with the teacher at all layers. This is consistent with many previous works that empirically show the network is learned in a bottom-up manner (Li et al., 2018).

Note that the alignment may happen *concurrently* across layers: if the activations of layer 1 start to align, then activations of layer 2, which depends on activations of layer 1, will also start to align since there now exists a W_2 that yields strong alignments, and so on. This creates a *critical path* from important student nodes at the lowest layer all the way to the output, and this critical path accelerates the convergence of that student node. We leave a formal analysis to the future work.

Deeper Student than Teacher. Note that both theorems only requires Assumption 1 be hold at $l = 1$, and it is fine to have identity mappings at “information passing” layers $l > 1$. Therefore,

when student network is deeper than teacher, by adding identity layers beyond the topmost layer on the teacher side, the conclusion of Theorem 4 still holds. This also suggests that the lowest layer of the student would match the lowest layer of the teacher, even if they have different number of layers.

4.5 SMALL GRADIENT CASE

We just analyze the ideal case in which we have infinite number of training samples (R_0 is a region), and have performed SGD for infinite iterations so that we could reach critical points in which $\mathbf{g}_l(\mathbf{x}) = \mathbf{0}$ for every $\mathbf{x} \in R_0$. A natural question arises. Are these conditions achievable in practice?

In practice, the gradient of SGD never reaches 0 but might fluctuate around (i.e., $\|\mathbf{g}_l(\mathbf{x})\|_\infty \leq \epsilon$). In this case, Theorem 5 shows that a rough recovery still follows. We now can see the ratio of recovery for weights/biases separately, as a function of ϵ . Note that here we separate weights and biases: $\mathbf{w}_j = [\tilde{\mathbf{w}}_j^\top, b_j]^\top$, and $\theta_{jj'}$ is the angle of two (bias-free) weights $\tilde{\mathbf{w}}_j$ and $\tilde{\mathbf{w}}_{j'}$.

Theorem 5 (Noisy Recovery). *If Assumption 1 holds and any two teachers \mathbf{w}_j^* , $\mathbf{w}_{j'}^*$ satisfy $\tilde{\theta}_{jj'} \geq \tilde{\theta}_0 > 0$ or $|b_{j'}^* - b_j^*| \geq b_0 > 0$. Suppose $\|\mathbf{g}_1(\mathbf{x}, \hat{\mathcal{W}})\|_\infty \leq \epsilon$ for any $\mathbf{x} \in R_0$ with $\epsilon \leq \epsilon_0$, then for any teacher j at $l = 1$, if there exists a region $R \in \mathcal{R}$ and a student observer k so that $\partial E_j^* \cap E_k \cap R \neq \emptyset$, and $\alpha_{kj}(R) \neq 0$, then j is roughly aligned with a student k' : $\sin \tilde{\theta}_{jk'} = \mathcal{O}\left(\frac{\epsilon^{1-\delta}}{|\alpha_{kj}|}\right)$ and $|b_j^* - b_{k'}| = \mathcal{O}\left(\frac{\epsilon^{1-2\delta}}{|\alpha_{kj}|}\right)$ for any $\delta > 0$. The hidden constants depends on δ , ϵ_0 and the size of region $\partial E_j^* \cap E_k \cap R$.*

Although the proof of Theorem 5 still assumes infinite number of data points, in the proof only a discrete set of data points are important to complete the proof by contradiction. Identifying these data points would lead to a formal generalization bound. That is, if training with finite number of samples of a specific distribution, we would obtain a certain generalization performance. For this we leave it to future work.

5 ANALYSIS ON TRAINING DYNAMICS

From the previous analysis, we see at SGD critical points, under mild conditions, each teacher node will be aligned with at least one student node. This would naturally yields low generalization error.

A natural question arise: is “running SGD long enough” a sufficient condition to achieve these critical points? Previous works (Ge et al., 2017; Livni et al., 2014) show that empirically SGD does not recover the parameters of a teacher network up to permutation.

There are several reasons. First, from Theorem 3, there exist student nodes that are not aligned with the teacher, so a simple permutation test on student weights might fail. Second, as suggested by Theorem 5, to recover a teacher node k with small α_{kj} (and thus small $\|\mathbf{v}_k^*\|$ since $\alpha_{kj} = \mathbf{v}_k^{*\top} \mathbf{v}_j$), the SGD gradient bound ϵ needs to be very small, which means we would need to run SGD for a very long time. In fact, if $\mathbf{v}_k^* = \mathbf{0}$ then the teacher node k has no contribution to the output and reconstruction never happens. This is particularly problematic if the output dimension is 1 (scalar output), since a single small teacher weight v_k^* would block the recovery of the entire teacher node k . Given a finite number of iterations, how much the student is aligned with the teacher implicitly suggests the generalization performance.

In the following, as a starting point, we analyze the training dynamics of 2-layer network where V_1 and V_1^* are all constant. Here $\alpha_k = V_l^{*\top} \mathbf{v}_k$, $\beta_k = V_l^\top \mathbf{v}_k$ and $\mathbf{e}_l = V_l^* \mathbf{f}_l^* - V_l \mathbf{f}_l \in \mathbb{R}^C$ is the residue.

$$\dot{\mathbf{w}}_k = \mathbb{E}_{\mathbf{x}} [\mathbf{f}_{l-1} z_k [\mathbf{f}_l^{*\top} \alpha_k - \mathbf{f}_l^\top \beta_k]] = \mathbb{E}_{\mathbf{x}} [\mathbf{f}_{l-1} z_k [V_l^* \mathbf{f}_l^* - V_l \mathbf{f}_l]^\top \mathbf{v}_k] = \mathbb{E}_{\mathbf{x}} [\mathbf{f}_{l-1} z_k \mathbf{e}_l^\top \mathbf{v}_k] \quad (5)$$

We formally define the notion of strong or weak teacher node as follows. As in Section 4.2, without loss of generality, for layer $l = 1$, we set teacher $\|\mathbf{w}_j^*\|_2 = 1$ (bias included in l^2 norm).

Definition 4. *A teacher node j is strong (or weak), if $\|\mathbf{v}_j^*\|$ is large (or small). See Fig. 6(a).*

5.1 WEIGHT MAGNITUDE

From Eqn. 5, we know that for both ReLU and linear network (since $f_k(\mathbf{x}) = z_k(\mathbf{x})\mathbf{w}_k^\top \mathbf{f}_{l-1}(\mathbf{x})$):

$$\frac{1}{2} \frac{d\|\mathbf{w}_k\|^2}{dt} = \mathbf{w}_k^\top \dot{\mathbf{w}}_k = \mathbb{E}_{\mathbf{x}} [f_k \mathbf{r}_l^\top \mathbf{v}_k] \quad (6)$$

When there is only a single output, $C = 1$, \mathbf{r}_l is a scalar and Eqn. 6 is simply an inner product between the residue and the activation of node k , over the batch. So if the node k has activation which aligns well with the residual, the inner product is larger and $\|\mathbf{w}_k\|$ grows faster.

Relationship to techniques to compare network representations. Singular Vector Canonical Correlation Analysis (SVCCA) by Raghu et al. (2017) proposes to compare the intermediate representation of networks trained with different initialization: first perform SVD decomposition on $\mathbf{f}_l(\mathbf{x}_i) \in \mathbb{R}^{n_l \times N}$, where N is the number of data point in evaluation, to find the major left singular space, and then linearly project the spaces from two networks to a common subspace using CCA. From our perspective, the reason why it works is quite clear: first SVD step removes those unaligned student activations, since their magnitudes are often small due to Eqn. 6; then CCA step merges co-linear student nodes and removes the permutation ambiguity.

5.2 SIMPLIFICATION OF DYNAMICS

To further understand the dynamics, in particular to see that \mathbf{w}_k converge to any teacher node \mathbf{w}_j^* rather than just increase its norm, let's check one term $\alpha_{kj} \mathbf{f}_{l-1} z_k f_j^*$ in $\dot{\mathbf{w}}_k$. Using $f_j^* = z_j^* \mathbf{w}_j^{*\top} \mathbf{f}_{l-1} = z_j^* \mathbf{w}_j^{*\top} \mathbf{f}_{l-1}$ for $l = 1$, we have:

$$\mathbb{E}_{\mathbf{x}} [\mathbf{f}_{l-1} z_k f_j^*] = \mathbb{E}_{\mathbf{x}} [\mathbf{f}_{l-1} z_k z_j^* \mathbf{f}_{l-1}^\top] \mathbf{w}_j^* = G_{kj} \mathbf{w}_j^* \quad (7)$$

where $G_{kj} = \mathbb{E}_{\mathbf{x}} [\mathbf{f}_{l-1} z_k z_j^* \mathbf{f}_{l-1}^\top]$. Putting it in another way, we want to check the spectrum property of the PSD matrix G_{kj} . Intuitively, the direction of $\mathbb{E}_{\mathbf{x}} [\mathbf{f}_{l-1} z_k f_j^*]$ should lie between \mathbf{w}_k and \mathbf{w}_j^* to push \mathbf{w}_k towards \mathbf{w}_j^* , and the magnitude is large when \mathbf{w}_k and \mathbf{w}_j^* are close to each other. This means that if \mathbf{r} is dominated by a teacher j (i.e., $\|\mathbf{v}_j^*\|$ is large), then $\dot{\mathbf{w}}_k$ would push \mathbf{w}_k towards \mathbf{w}_j^* . This also shows that SGD will first try fitting strong teacher nodes, then weak teacher nodes.

Theorem 6 confirms this intuition if \mathbf{f}_{l-1} follows spherical symmetric distribution (e.g., $\mathcal{N}(0, I)$).

Theorem 6. *If \mathbf{f}_{l-1} follows spherical symmetric distribution, then $\mathbb{E}_{\mathbf{x}} [\mathbf{f}_{l-1} z_k f_j^*] \propto \frac{\|\mathbf{w}_j^*\| \|\mathbf{w}_k\|}{2} [(\pi - \theta) \mathbf{w}_j^* + \sin \theta \mathbf{w}_k]$, where θ is the angle between \mathbf{w}_j^* and \mathbf{w}_k .*

As a result, for all $\theta \in [0, \pi]$, $\mathbb{E}_{\mathbf{x}} [\mathbf{f}_{l-1} z_k f_j^*]$ is always between \mathbf{w}_j^* and \mathbf{w}_k since $\pi - \theta$ and $\sin \theta$ are always non-negative. Without such symmetry, we assume the following holds:

Assumption 2. $\mathbb{E}_{\mathbf{x}} [\mathbf{f}_{l-1} z_k f_j] = \psi(\theta_{jk}) \mathbf{w}_j + \psi'(\theta_{jk}) \mathbf{w}_k$, where $\psi(\pi) = 0$.

Note that critical point analysis is applicable to any batch size, including 1. On the other hand, Assumption 2 holds when a moderately large batchsize leads to a decent estimation of the terms. Intuitively, the two help determine an optimal batchsize.

With Assumption 2, we can write the dynamics as $\dot{\mathbf{w}}_k = \|\mathbf{w}_k\| \mathbf{r}_k$, where the time-varying *per-node* residue \mathbf{r}_k of node k is defined as the following. Here ν is a scalar related to ψ' , and θ_{jk} is the angle (bias included) between \mathbf{w}_j and \mathbf{w}_k , no matter whether they are from teacher or student:

$$\mathbf{r}_k = \sum_j \alpha_{jk} \psi(\theta_{jk}) \mathbf{w}_j^* - \sum_{k'} \beta_{k'k} \psi(\theta_{k'k}) \mathbf{w}_{k'} - \nu \mathbf{w}_k \quad (8)$$

5.3 SYMMETRY BREAKING, WINNERS-TAKE-ALL AND FOCUS SHIFTING

Now we want to understand the simplified dynamics $\dot{\mathbf{w}}_k = \|\mathbf{w}_k\| \mathbf{r}_k$. Due to its non-linear nature and complicated behaviors, we provide an intuitive analysis to understand the nature of dynamics, and leave a formal analysis as the future work.

Let $\bar{\mathbf{w}} = \mathbf{w}/\|\mathbf{w}\|_2$. First, for two nodes $k \neq k'$, regardless of the form of \mathbf{r}_k , we have:

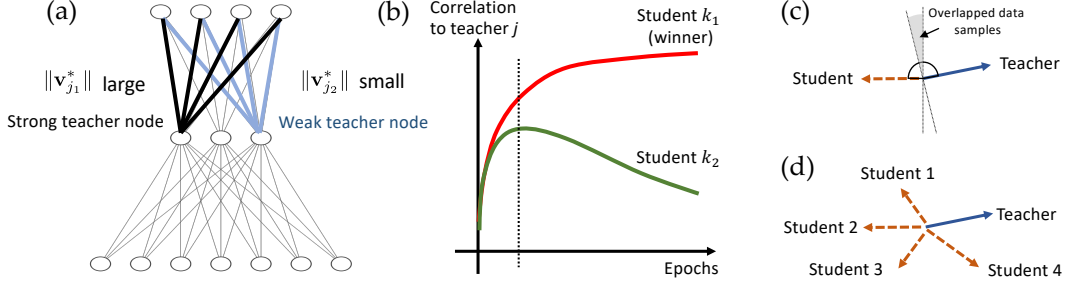


Figure 6: (a) Definition of strong (and weak) teacher nodes (Def. 4). (b) Focus shifting: after the strong teacher j was explained well, the student node k_2 moves to another teacher, yielding reduction of its correlation to teacher j . (c) In the worst case, it could take a long (or infinite amount of) time for the student to converge to a teacher, due to the scarcity of data points in both active regions, which drive the move. (d) Over-parameterization helps accelerate the convergence.

Theorem 7. For dynamics $\dot{\mathbf{w}}_k = \|\mathbf{w}_k\| \mathbf{r}_k$, we have $\frac{d}{dt} \ln \frac{\|\mathbf{w}_k\|}{\|\mathbf{w}_{k'}\|} = \bar{\mathbf{w}}_k^\top \mathbf{r}_k - \bar{\mathbf{w}}_{k'}^\top \mathbf{r}_{k'}$.

For a simple (and symmetric) case that $\mathbf{r}_k = \mathbf{r} = \mathbf{w}^* - \sum_k c_k \mathbf{w}_k$ with all $c_k > 0$, where \mathbf{w}^* is a joint contribution of all teacher nodes, we could show that (in the proof of Theorem 7), when $\bar{\mathbf{w}}_k^\top \mathbf{r}_k > \bar{\mathbf{w}}_{k'}^\top \mathbf{r}_{k'}$, $\frac{d}{dt} (\bar{\mathbf{w}}_k^\top \mathbf{r}_k - \bar{\mathbf{w}}_{k'}^\top \mathbf{r}_{k'}) < 0$ and vice versa. So the system provides negative feedback until $\bar{\mathbf{w}}_k = \bar{\mathbf{w}}_{k'}$ and according to Eqn. 7, the ratio between $\|\mathbf{w}_k\|$ and $\|\mathbf{w}_{k'}\|$ remains constant, after initial transition. We can also show that $\bar{\mathbf{w}}_k$ will align with \mathbf{w}^* and every student node goes to \mathbf{w}^* .

However, due to Theorem 6, the net effect \mathbf{w}^* can be *different* for different students and thus \mathbf{r}_k are different. This opens the door for complicated dynamic behavior of neural network training.

Symmetry breaking. As one example, if we add a very small delta to some node, say to $k = 1$ so that $\mathbf{r}_1 = \mathbf{r} + \epsilon \mathbf{w}^*$. Then to reach a stationary point $\frac{d}{dt} (\bar{\mathbf{w}}_k^\top \mathbf{r}_k - \bar{\mathbf{w}}_{k'}^\top \mathbf{r}_{k'}) = 0$, we have $\bar{\mathbf{w}}_k^\top \mathbf{r}_k > \bar{\mathbf{w}}_{k'}^\top \mathbf{r}_{k'}$ and thus according to Theorem 7, $\|\mathbf{w}_k\|/\|\mathbf{w}_{k'}\|$ grows exponentially (see details in the proof of Theorem 7). This symmetric breaking behavior provides a potential *winners-take-all* mechanism, since according to Theorem 6, the coefficient of \mathbf{w}^* depends critically on the initial angle between \mathbf{w}_k and \mathbf{w}^* .

Strong teacher nodes are learned first. If $\|\mathbf{v}_j^*\|$ is the largest among teacher nodes, then for any k , their $|\alpha_{jk}| \gg |\alpha_{j'k}|$ for other teacher j' . According to Eqn. 8 thus \mathbf{r}_k heavily biases towards \mathbf{w}_j^* . Following the analysis above, all student nodes move towards teacher j . As a result, strong teacher learns first and is often covered by multiple co-linear students (Fig. 8, teacher-1).

Focus shifting to weak teacher nodes. The process above continues until residual along the direction of \mathbf{w}_j^* quickly shrinks and residual corresponding to other teacher node (e.g., $\mathbf{w}_{j'}^*$ for $j' \neq j$) becomes dominant. Since each \mathbf{r}_k is different, student node k whose direction is closer to $\mathbf{w}_{j'}^*$ ($j' \neq j$) will shift their focus towards $\mathbf{w}_{j'}^*$ (Fig. 6(b)) This is shown in the green (shift to teacher-3) and magenta (shift to teacher-5) curves in one of the simulations (Fig. 8, first row).

Possible slow convergence to weak teacher nodes. While expected angle between two weights from random initialization is $\pi/2$, shifting a student node \mathbf{w}_k from chasing after a strong teacher node \mathbf{w}_j^* to a weaker one $\mathbf{w}_{j'}^*$, could yield a large initial angle (e.g., close to π) between \mathbf{w}_k and $\mathbf{w}_{j'}^*$. For example, all student nodes have been attracted to the opposite direction of a weak teacher node. In this case, the convergence can be arbitrarily slow.

In the following we give one concrete worst case example (Fig. 6(c)). Suppose we only have one student k . Let $P_{\mathbf{w}_k}^\perp = I_{(d+1) \times (d+1)} - \bar{\mathbf{w}}_k \bar{\mathbf{w}}_k^\top \in \mathbb{R}^{(d+1) \times (d+1)}$ be the orthogonal complement projection operator. Note that $\frac{d}{dt} \bar{\mathbf{w}}_k = P_{\mathbf{w}_k}^\perp \mathbf{r}_k$ (Eqn. 66 in Appendix) and $P_{\mathbf{w}_k}^\perp \mathbf{w}_k = \mathbf{0}$. From Eqn. 8 we have:

$$\frac{d}{dt} (\mathbf{w}_j^* \bar{\mathbf{w}}_k) = \mathbf{w}_j^* P_{\mathbf{w}_k}^\perp \mathbf{r}_k = \alpha_{jk} \psi(\theta_{jk}) \mathbf{w}_j^* P_{\mathbf{w}_k}^\perp \mathbf{w}_j^* = \alpha_{jk} \psi(\theta_{jk}) \sin^2 \theta_{jk} \quad (9)$$

On the other hand, $\frac{d}{dt} (\mathbf{w}_j^* \bar{\mathbf{w}}_k) = \frac{d}{dt} \cos \theta_{jk} = -\sin \theta_{jk} \dot{\theta}_{jk}$. So we arrive at

$$\dot{\theta}_{jk} = -\alpha_{jk} \psi(\theta_{jk}) \sin \theta_{jk} \quad (10)$$

Since $\psi(\theta_{jk}) \sin \theta_{jk} \sim (\pi - \theta_{jk})^2$ around $\theta_{jk} = \pi$, the time spent from $\theta_{jk} = \pi - \epsilon$ to some θ_0 is $t_0 \sim \frac{1}{\epsilon} - \frac{1}{\pi - \theta_0} \rightarrow +\infty$ when $\epsilon \rightarrow 0$. Therefore, it takes infinite time for the student k to converge to teacher j .

The role played by over-parameterization. In this case, over-parameterization helps by having more student nodes that are possibly ready for shifting towards weaker teachers, and thus accelerate convergence (Fig. 12). Alternatively, we could reinitialize those student nodes (Prakash et al., 2019).

Connection to Competitive Lotka-Volterra equations. The training dynamics is related to Competitive Lotka-Volterra equations (Smale, 1976; Zhu & Yin, 2009; Hosono, 1998), which has been extensively used to model the dynamics of multiple species competing over limited resources in a biological system. In our setting, the teacher nodes are the “resources” and the student nodes are the “species”. The main difference here is that there are multiple teacher nodes that are not mutually replaceable, and a certain kind of resource becomes more important if one species have already obtained a lot of it. This leads to neuron specialization (Saad & Solla, 1996; 1995).

6 EXPERIMENTS

Setup. For two-layered network, we use vanilla SGD with learning rate 0.01 and batchsize 16 to train the model. $C = 50$ and input dimension $d = m_0 = n_0 = 100$. Each epoch contains 1k minibatches. For multi-layered network, we use 50-75-100-125 (i.e., $m_1 = 50, m_2 = 75, m_3 = 100, m_4 = 125, L = 5, d = m_0 = n_0 = 100$ and $C = m_5 = n_5 = 50$). The input distribution follows $\mathcal{N}(0, \sigma^2 I)$ with $\sigma = 1.5$ and we sample 10000 as the training set and another 10000 as the evaluation. The teacher network is constructed to satisfy Assumption 1 for all layers: at each layer, teacher filters are distinct from each other and their bias is set so that $\sim 50\%$ of the input data activates the nodes. This makes their boundary (maximally) visible in the dataset. Experiments on CIFAR10 uses 64-64-64-64 ConvNet (64 are channel sizes of the hidden layers, $L = 5$). The teacher network is pre-trained on CIFAR10 training set and was pruned in a structured manner to keep strong teacher nodes. The student is over-parameterized based on teacher’s remaining channels.

Strong/weak teacher node. To check the convergence behavior, we set up a diverse strength of teacher nodes. For teacher j , we make $\|\mathbf{v}_j^*\| \sim 1/j^p$, where p is the *teacher polarity factor* that controls how strong the energy decays across different teacher nodes. $p = 0$ means all teacher nodes are symmetric, and large p means that the strength of teacher nodes are more polarized.

6.1 THE ALIGNMENT AND FAN-OUT WEIGHTS

First we verify Theorem 2 and Theorem 3 in the 2-layer setting. Fig. 8 shows student nodes correlate with different teacher nodes over time. Fig. 7 shows for different degrees of over-parameterization (1x/2x/5x/10x), for nodes that do not align with the teacher nodes (i.e., normalized correlation to the most correlated teacher is low), their magnitudes of fan-out weights are small. Otherwise the nodes which align well with some teacher node have high fan-out weights.

Similar phenomenon happens in multi-layered setting (Fig. 9). For each student node k , the x-axis is its best normalized correlation to teacher nodes, and y-axis is $\sqrt{\mathbb{E}_{\mathbf{x}} [\beta_{kk}(\mathbf{x})]}$, which is equivalent to $\|\mathbf{v}_k\|$ in 2-layer case. From the same figure, we can also see the lowest layer learns first (the “L-shape” curve was established at epoch 10), then the top layers follow.

6.2 THE EFFECT OF OVER-PARAMETERIZATION

We plot the average rate of a teacher node that is matched with at least one student node successfully (i.e., correlation > 0.95). Fig. 10 shows that stronger teacher nodes are more likely to be matched, while weaker ones may not be explained well, in particular when the strength of the teacher nodes are polarized (p is large). Over-parameterized student can explain more teacher nodes, while 1x parameterization that has sufficient capacity to fit the teacher perfectly, gets stuck despite long training.

Note that from the loss curve (Fig. 11), the difference is not large since weak teacher nodes do not substantially affect final loss. However, to achieve state-of-the-art performance on the real dataset, grabbing every weak teacher node can be important.

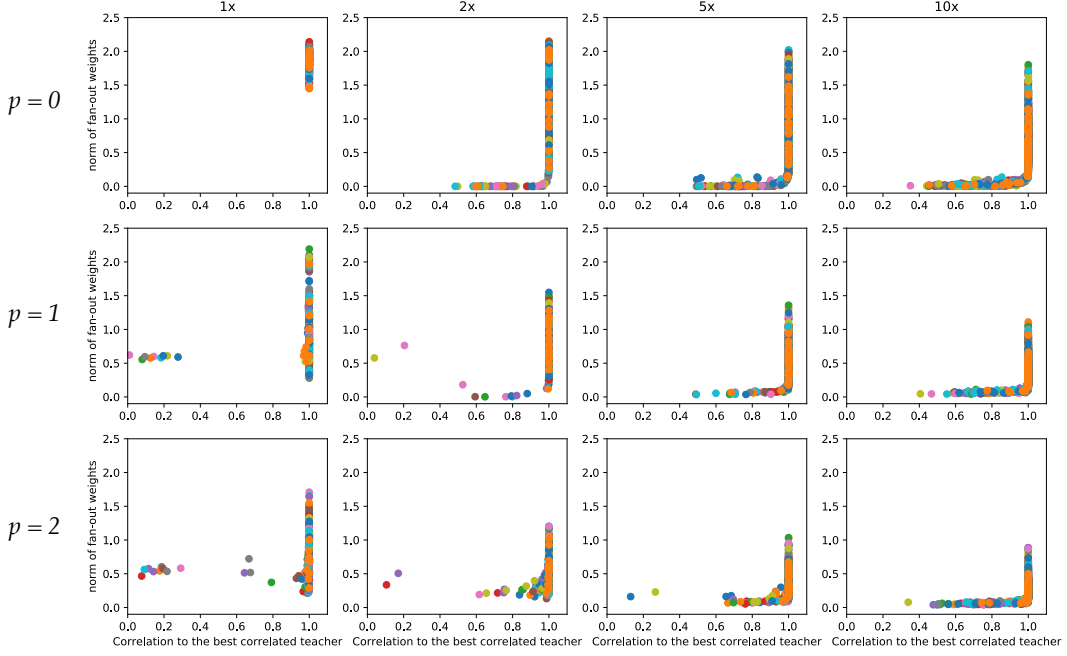


Figure 7: Convergence of a 2-layered network with 10 teacher nodes and 1x/2x/5x/10x student nodes. p is teacher polarity factor. For a student node k , we plot its normalized correlation to its best correlated teacher as the x coordinate and the fan-out weight norm $\|\mathbf{v}_k\|$ as the y coordinate. We plot results from 32 random seed. Student nodes of different seeds are in different color. A “useless” student node that has low correlations with teachers and low fan-out weight norm (Theorem 3). Higher p makes reconstruction of teacher node harder, in particular if the student network is not over-parameterized.

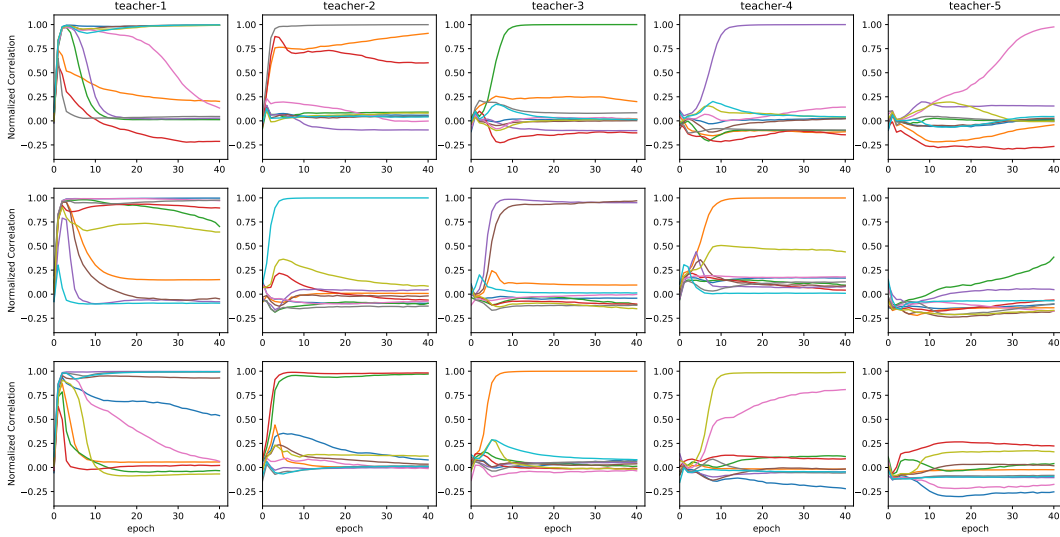


Figure 8: Convergence of student nodes with teacher polarity $p = 1$. Same students are represented by the same color across plots. Three rows represent three different random seeds. We can see more students nodes converge to teacher-1 first. In contrast, teacher-5 was not explained until later by a node (e.g., magenta in the first row) that first chases after teacher-1 then shifts its focus.

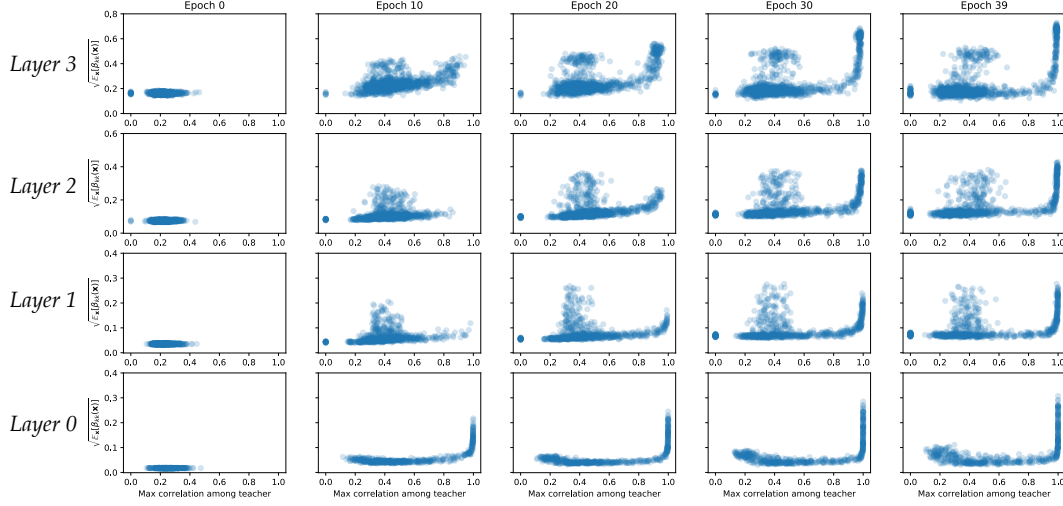


Figure 9: Student maximal correlation versus their fan-out coefficients in 4 layer network. Hidden layer dimensions of the teacher is 50-75-100-125. Student is 10x over-parameterization. For node k , y-axis is $\sqrt{\mathbb{E}_{\mathbf{x}} [\beta_{kk}(\mathbf{x})]}$, which equivalent to the fan-out weight norm $\|\mathbf{v}_k\|$ in 2-layer case, and x-axis is its max correlation to the teachers. We can clear see the lower layer learns first.

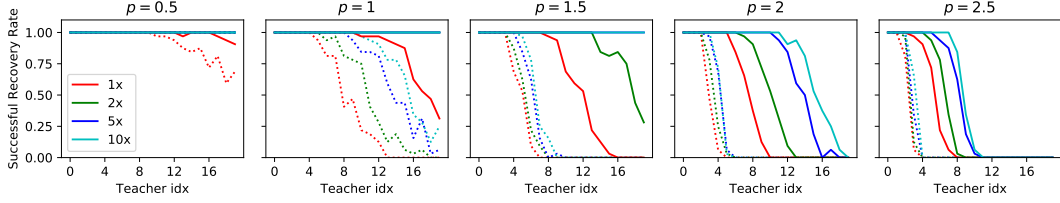


Figure 10: Success rate (over 32 trials with different random seeds) of recovery of 20 teacher nodes on 2-layer network at different teacher polarity p and different over-parameterization. Dotted line: successful rate after 5 epochs. Solid line: successful rate after 100 epochs.

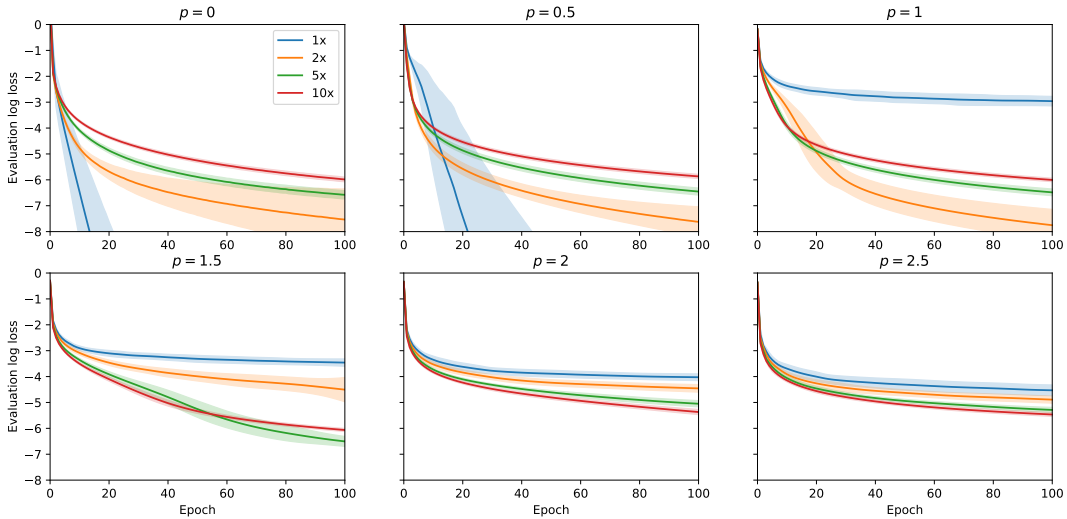


Figure 11: Evaluation loss convergence curve with different teacher polarity p . When p becomes higher, 1x parameterization becomes worse than over-parameterization.

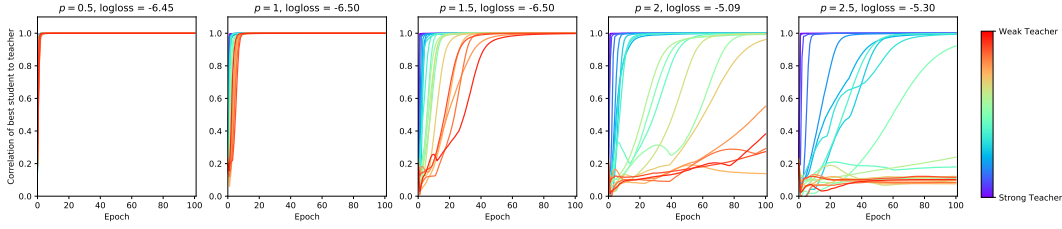


Figure 12: Evolution of best student correlation to teacher over iterations. Each rainbow color represents one of the 20 teachers (blue: strongest, red: weakest). 5x over-parameterization on 2-layer network.

Besides the final matching rate, the convergence speed of student nodes (Fig. 12) towards different teacher node is also very different. Many student nodes converge to a strong teacher node. Once the strong teacher node was covered well, weaker teacher nodes are covered after many epochs.

In CIFAR10, the convergence behavior of student network is shown in Fig. 13. Over-parameterization boosts the teacher-student alignments, measured by mean of maximal normalized correlation $\rho_{\text{mean}} = \text{mean}_{j \in \text{teacher}} \max_{j' \in \text{student}} \tilde{\mathbf{f}}_j^* \tilde{\mathbf{f}}_{j'}$ at each layer ($\tilde{\mathbf{f}}_j$ is the normalized activation of node j over N evaluation samples), and improves the generalization.

7 CONCLUSION AND FUTURE WORK

In this paper, we use student-teacher setting to analyze how an (over-parameterized) deep ReLU student network trained with SGD learns from the output of a teacher. When the magnitude of gradient per sample is small (student weights are near the critical points), the teacher can be proven to be covered by (possibly multiple) students and thus the teacher network is recovered in the lowest layer. By analyzing training dynamics, we also show that strong teacher node with large $\|\mathbf{v}^*\|$ is reconstructed first, while weak teacher node is reconstructed slowly. This reveals one important reason why the training takes long to reconstruct all teacher weights and why generalization improves with more training.

Our analysis might help address the following apparent contradiction in neural network training: on one hand, over-parameterization helps generalization; on the other hand, works on model pruning (LeCun et al., 1990; Liu et al., 2019; Hu et al., 2016; Han et al., 2015) shows there are a lot of parameter redundancy in trained deep model and recent lottery ticket hypothesis (Frankle & Carbin, 2019; Frankle et al., 2019; Zhou et al., 2019; Morcos et al., 2019) shows that a subnetwork in the trained model, if trained alone, could achieve comparable or even better generalization. Based on our analysis, the intuition to explain both sides of the empirical evidences is that a good initialization is important but hard to find, and over-parameterization can help compensate for that by creating more observers (Theorem 4) and accelerating the focus shifting (Sec. 5.3). Due to the symmetry breaking property (Sec. 5.3), small changes in the initialization could lead to huge difference in the learned weight. Therefore, it is unlikely to directly find the *lucky weights* or *winning tickets* at initialization, until after the symmetry breaking happens. We leave the formal analysis regarding to initialization to the future work.

As the next step, we would like to extend our analysis to finite sample case, and analyze the training dynamics in a more formal way. Verifying the insights from theoretical analysis on a large dataset (e.g., ImageNet) is also the next step.

8 ACKNOWLEDGEMENT

I thank Banghua Zhu, Xiaoxia (Shirley) Wu, Lexing Ying, Jonathan Frankle and Ari Morcos for insightful discussions.

REFERENCES

Zeyuan Allen-Zhu, Yuanzhi Li, and Yingyu Liang. Learning and generalization in overparameterized neural networks, going beyond two layers. *NeurIPS*, 2019a.

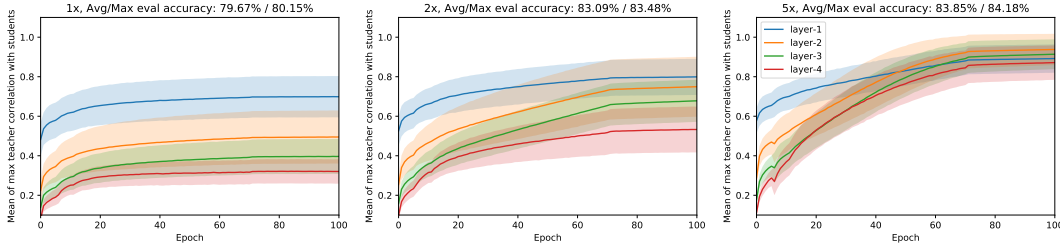


Figure 13: Mean of the max teacher correlation ρ_{mean} with student nodes over epochs in CIFAR10. More over-parameterization gives better teacher-student alignment across all layers and achieves strong generalization.

Zeyuan Allen-Zhu, Yuanzhi Li, and Zhao Song. A convergence theory for deep learning via over-parameterization. In Kamalika Chaudhuri and Ruslan Salakhutdinov (eds.), *Proceedings of the 36th International Conference on Machine Learning*, volume 97 of *Proceedings of Machine Learning Research*, pp. 242–252, Long Beach, California, USA, 09–15 Jun 2019b. PMLR. URL <http://proceedings.mlr.press/v97/allen-zhu19a.html>.

Raef Bassily, Mikhail Belkin, and Siyuan Ma. On exponential convergence of sgd in non-convex over-parametrized learning. *arXiv preprint arXiv:1811.02564*, 2018.

Dimitri P Bertsekas and John N Tsitsiklis. Gradient convergence in gradient methods with errors. *SIAM Journal on Optimization*, 10(3):627–642, 2000.

Léon Bottou. Large-scale machine learning with stochastic gradient descent. In *Proceedings of COMPSTAT'2010*, pp. 177–186. Springer, 2010.

Yuan Cao and Quanquan Gu. Generalization bounds of stochastic gradient descent for wide and deep neural networks. *arXiv preprint arXiv:1905.13210*, 2019.

Pratik Chaudhari and Stefano Soatto. Stochastic gradient descent performs variational inference, converges to limit cycles for deep networks. In *2018 Information Theory and Applications Workshop (ITA)*, pp. 1–10. IEEE, 2018.

Pratik Chaudhari, Anna Choromanska, Stefano Soatto, Yann LeCun, Carlo Baldassi, Christian Borgs, Jennifer Chayes, Levent Sagun, and Riccardo Zecchina. Entropy-sgd: Biasing gradient descent into wide valleys. *ICLR*, 2017.

Lenaic Chizat and Francis Bach. On the global convergence of gradient descent for over-parameterized models using optimal transport. In *Advances in neural information processing systems*, pp. 3036–3046, 2018.

Hadi Daneshmand, Jonas Kohler, Aurelien Lucchi, and Thomas Hofmann. Escaping saddles with stochastic gradients. *arXiv preprint arXiv:1803.05999*, 2018.

Jacob Devlin, Ming-Wei Chang, Kenton Lee, and Kristina Toutanova. Bert: Pre-training of deep bidirectional transformers for language understanding. *arXiv preprint arXiv:1810.04805*, 2018.

Simon S Du, Chi Jin, Jason D Lee, Michael I Jordan, Aarti Singh, and Barnabas Poczos. Gradient descent can take exponential time to escape saddle points. In *Advances in neural information processing systems*, pp. 1067–1077, 2017.

Simon S Du, Jason D Lee, Yuandong Tian, Barnabas Poczos, and Aarti Singh. Gradient descent learns one-hidden-layer cnn: Don’t be afraid of spurious local minima. *ICML*, 2018.

Simon S Du, Jason D Lee, Haochuan Li, Liwei Wang, and Xiyu Zhai. Gradient descent finds global minima of deep neural networks. *ICML*, 2019.

Jonathan Frankle and Michael Carbin. The lottery ticket hypothesis: Training pruned neural networks. *ICLR*, 2019.

- Jonathan Frankle, Gintare Karolina Dziugaite, Daniel M Roy, and Michael Carbin. The lottery ticket hypothesis at scale. *arXiv preprint arXiv:1903.01611*, 2019.
- Jason AS Freeman and David Saad. Online learning in radial basis function networks. *Neural Computation*, 9(7):1601–1622, 1997.
- Rong Ge, Furong Huang, Chi Jin, and Yang Yuan. Escaping from saddle pointsonline stochastic gradient for tensor decomposition. In *Conference on Learning Theory*, pp. 797–842, 2015.
- Rong Ge, Jason D Lee, and Tengyu Ma. Learning one-hidden-layer neural networks with landscape design. *arXiv preprint arXiv:1711.00501*, 2017.
- Sebastian Goldt, Madhu S Advani, Andrew M Saxe, Florent Krzakala, and Lenka Zdeborová. Dynamics of stochastic gradient descent for two-layer neural networks in the teacher-student setup. *NeurIPS*, 2019.
- Song Han, Jeff Pool, John Tran, and William Dally. Learning both weights and connections for efficient neural network. In *Advances in neural information processing systems*, pp. 1135–1143, 2015.
- Babak Hassibi, David G Stork, and Gregory J Wolff. Optimal brain surgeon and general network pruning. In *IEEE international conference on neural networks*, pp. 293–299. IEEE, 1993.
- Elad Hazan and Satyen Kale. Beyond the regret minimization barrier: optimal algorithms for stochastic strongly-convex optimization. *The Journal of Machine Learning Research*, 15(1): 2489–2512, 2014.
- Kaiming He, Xiangyu Zhang, Shaoqing Ren, and Jian Sun. Deep residual learning for image recognition. In *Proceedings of the IEEE conference on computer vision and pattern recognition*, pp. 770–778, 2016.
- Sepp Hochreiter and Jürgen Schmidhuber. Flat minima. *Neural Computation*, 9(1):1–42, 1997.
- Kurt Hornik, Maxwell Stinchcombe, and Halbert White. Multilayer feedforward networks are universal approximators. *Neural networks*, 2(5):359–366, 1989.
- Yuzo Hosono. The minimal speed of traveling fronts for a diffusive lotka-volterra competition model. *Bulletin of Mathematical Biology*, 60(3):435–448, 1998.
- Hengyuan Hu, Rui Peng, Yu-Wing Tai, and Chi-Keung Tang. Network trimming: A data-driven neuron pruning approach towards efficient deep architectures. *arXiv preprint arXiv:1607.03250*, 2016.
- Arthur Jacot, Franck Gabriel, and Clément Hongler. Neural tangent kernel: Convergence and generalization in neural networks. In *Advances in neural information processing systems*, pp. 8571–8580, 2018.
- Chi Jin, Rong Ge, Praneeth Netrapalli, Sham M Kakade, and Michael I Jordan. How to escape saddle points efficiently. In *Proceedings of the 34th International Conference on Machine Learning-Volume 70*, pp. 1724–1732. JMLR. org, 2017.
- Kenji Kawaguchi. Deep learning without poor local minima. In *Advances in neural information processing systems*, pp. 586–594, 2016.
- Rohith Kuditipudi, Xiang Wang, Holden Lee, Yi Zhang, Zhiyuan Li, Wei Hu, Sanjeev Arora, and Rong Ge. Explaining landscape connectivity of low-cost solutions for multilayer nets. *CoRR*, abs/1906.06247, 2019. URL <http://arxiv.org/abs/1906.06247>.
- Thomas Laurent and James Brecht. Deep linear networks with arbitrary loss: All local minima are global. In *International Conference on Machine Learning*, pp. 2908–2913, 2018.
- Thomas Laurent and James von Brecht. The multilinear structure of relu networks. *arXiv preprint arXiv:1712.10132*, 2017.

- Yann LeCun, John S Denker, and Sara A Solla. Optimal brain damage. In *Advances in neural information processing systems*, pp. 598–605, 1990.
- Chunyuan Li, Heerad Farkhoor, Rosanne Liu, and Jason Yosinski. Measuring the intrinsic dimension of objective landscapes. *ICLR*, 2018.
- Yuanzhi Li and Yingyu Liang. Learning overparameterized neural networks via stochastic gradient descent on structured data. In *Advances in Neural Information Processing Systems*, pp. 8157–8166, 2018.
- Chaoyue Liu and Mikhail Belkin. Mass: an accelerated stochastic method for over-parametrized learning. *arXiv preprint arXiv:1810.13395*, 2018.
- Zhuang Liu, Mingjie Sun, Tinghui Zhou, Gao Huang, and Trevor Darrell. Rethinking the value of network pruning. In *International Conference on Learning Representations*, 2019. URL <https://openreview.net/forum?id=rJlnB3C5Ym>.
- Roi Livni, Shai Shalev-Shwartz, and Ohad Shamir. On the computational efficiency of training neural networks. In *Advances in neural information processing systems*, pp. 855–863, 2014.
- Siyuan Ma, Raef Bassily, and Mikhail Belkin. The power of interpolation: Understanding the effectiveness of sgd in modern over-parametrized learning. *arXiv preprint arXiv:1712.06559*, 2017.
- CWH Mace and ACC Coolen. Statistical mechanical analysis of the dynamics of learning in perceptrons. *Statistics and Computing*, 8(1):55–88, 1998.
- Stephan Mandt, Matthew D Hoffman, and David M Blei. Stochastic gradient descent as approximate bayesian inference. *The Journal of Machine Learning Research*, 18(1):4873–4907, 2017.
- Gaétan Marceau-Caron and Yann Ollivier. Natural langevin dynamics for neural networks. In *International Conference on Geometric Science of Information*, pp. 451–459. Springer, 2017.
- Ari S Morcos, Haonan Yu, Michela Paganini, and Yuandong Tian. One ticket to win them all: generalizing lottery ticket initializations across datasets and optimizers. *NeurIPS*, 2019.
- Behnam Neyshabur, Ruslan R Salakhutdinov, and Nati Srebro. Path-sgd: Path-normalized optimization in deep neural networks. In *Advances in Neural Information Processing Systems*, pp. 2422–2430, 2015.
- Quynh Nguyen and Matthias Hein. The loss surface of deep and wide neural networks. In *Proceedings of the 34th International Conference on Machine Learning-Volume 70*, pp. 2603–2612. JMLR. org, 2017.
- Aaditya Prakash, James Storer, Dinei Florencio, and Cha Zhang. Repr: Improved training of convolutional filters. In *Proceedings of the IEEE Conference on Computer Vision and Pattern Recognition*, pp. 10666–10675, 2019.
- Maithra Raghu, Justin Gilmer, Jason Yosinski, and Jascha Sohl-Dickstein. Svcca: Singular vector canonical correlation analysis for deep learning dynamics and interpretability. In *Advances in Neural Information Processing Systems*, pp. 6076–6085, 2017.
- David Saad and Sara A Solla. On-line learning in soft committee machines. *Physical Review E*, 52(4):4225, 1995.
- David Saad and Sara A Solla. Dynamics of on-line gradient descent learning for multilayer neural networks. In *Advances in neural information processing systems*, pp. 302–308, 1996.
- Itay Safran and Ohad Shamir. Spurious local minima are common in two-layer relu neural networks. *arXiv preprint arXiv:1712.08968*, 2017.
- Christopher J Shallue, Jaehoon Lee, Joe Antognini, Jascha Sohl-Dickstein, Roy Frostig, and George E Dahl. Measuring the effects of data parallelism on neural network training. *Journal of Machine Learning Research (JMLR)*, 2018.

- David Silver, Aja Huang, Chris J Maddison, Arthur Guez, Laurent Sifre, George Van Den Driessche, Julian Schrittwieser, Ioannis Antonoglou, Veda Panneershelvam, Marc Lanctot, et al. Mastering the game of go with deep neural networks and tree search. *nature*, 529(7587):484, 2016.
- Steve Smale. On the differential equations of species in competition. *Journal of Mathematical Biology*, 3(1):5–7, 1976.
- Yuandong Tian. An analytical formula of population gradient for two-layered relu network and its applications in convergence and critical point analysis. In *Proceedings of the 34th International Conference on Machine Learning-Volume 70*, pp. 3404–3413. JMLR. org, 2017.
- Yuandong Tian, Tina Jiang, Qucheng Gong, and Ari Morcos. Luck matters: Understanding training dynamics of deep relu networks. *arXiv preprint arXiv:1905.13405*, 2019.
- Max Welling and Yee W Teh. Bayesian learning via stochastic gradient langevin dynamics. In *Proceedings of the 28th international conference on machine learning (ICML-11)*, pp. 681–688, 2011.
- Lei Wu, Chao Ma, and E Weinan. How sgd selects the global minima in over-parameterized learning: A dynamical stability perspective. In *Advances in Neural Information Processing Systems*, pp. 8279–8288, 2018.
- Chulhee Yun, Suvrit Sra, and Ali Jadbabaie. Global optimality conditions for deep neural networks. In *International Conference on Learning Representations*, 2018. URL <https://openreview.net/forum?id=BJk7Gf-CZ>.
- Chulhee Yun, Suvrit Sra, and Ali Jadbabaie. Small nonlinearities in activation functions create bad local minima in neural networks. In *International Conference on Learning Representations*, 2019. URL https://openreview.net/forum?id=rke_YiRct7.
- Chiyuan Zhang, Samy Bengio, Moritz Hardt, Benjamin Recht, and Oriol Vinyals. Understanding deep learning requires rethinking generalization. *ICLR*, 2017.
- Kai Zhong, Zhao Song, Prateek Jain, Peter L Bartlett, and Inderjit S Dhillon. Recovery guarantees for one-hidden-layer neural networks. In *Proceedings of the 34th International Conference on Machine Learning-Volume 70*, pp. 4140–4149. JMLR. org, 2017.
- Hattie Zhou, Janice Lan, Rosanne Liu, and Jason Yosinski. Deconstructing lottery tickets: Zeros, signs, and the supermask. *NeurIPS*, 2019.
- Chao Zhu and G Yin. On competitive lotka–volterra model in random environments. *Journal of Mathematical Analysis and Applications*, 357(1):154–170, 2009.
- Difan Zou and Quanquan Gu. An improved analysis of training over-parameterized deep neural networks. *NeurIPS*, 2019.
- Difan Zou, Yuan Cao, Dongruo Zhou, and Quanquan Gu. Stochastic gradient descent optimizes over-parameterized deep relu networks. *arXiv preprint arXiv:1811.08888*, 2018.

9 APPENDIX

9.1 LEMMA 1

Proof. We prove by induction. When $l = L$ we know that $\mathbf{g}_L(\mathbf{x}) = \mathbf{f}_L^*(\mathbf{x}) - \mathbf{f}_L(\mathbf{x})$, by setting $V_L^*(\mathbf{x}) = V_L(\mathbf{x}) = I_{C \times C}$ and the fact that $D_L(\mathbf{x}) = I_{C \times C}$ (no ReLU gating in the last layer), the condition holds.

Now suppose for layer l , we have:

$$\mathbf{g}_l(\mathbf{x}) = D_l(\mathbf{x}) [A_l(\mathbf{x}) \mathbf{f}_l^*(\mathbf{x}) - B_l(\mathbf{x}) \mathbf{f}_l(\mathbf{x})] \quad (11)$$

$$= D_l(\mathbf{x}) V_l^\top(\mathbf{x}) [V_l^*(\mathbf{x}) \mathbf{f}_l^*(\mathbf{x}) - V_l(\mathbf{x}) \mathbf{f}_l(\mathbf{x})] \quad (12)$$

Using

$$\mathbf{f}_l(\mathbf{x}) = D_l(\mathbf{x}) W_l^\top \mathbf{f}_{l-1}(\mathbf{x}) \quad (13)$$

$$\mathbf{f}_l^*(\mathbf{x}) = D_l^*(\mathbf{x}) W_l^{*\top} \mathbf{f}_{l-1}^*(\mathbf{x}) \quad (14)$$

$$\mathbf{g}_{l-1}(\mathbf{x}) = D_{l-1}(\mathbf{x}) W_l \mathbf{g}_l(\mathbf{x}) \quad (15)$$

we have:

$$\mathbf{g}_{l-1}(\mathbf{x}) = D_{l-1}(\mathbf{x}) W_l \mathbf{g}_l(\mathbf{x}) \quad (16)$$

$$= D_{l-1}(\mathbf{x}) \underbrace{W_l D_l(\mathbf{x}) V_l^\top(\mathbf{x})}_{V_{l-1}^\top(\mathbf{x})} [V_l^*(\mathbf{x}) \mathbf{f}_l^*(\mathbf{x}) - V_l(\mathbf{x}) \mathbf{f}_l(\mathbf{x})] \quad (17)$$

$$= D_{l-1}(\mathbf{x}) V_{l-1}^\top(\mathbf{x}) \left[\underbrace{V_l^*(\mathbf{x}) D_l^*(\mathbf{x}) W_l^{*\top}}_{V_{l-1}^{*\top}(\mathbf{x})} \mathbf{f}_{l-1}^*(\mathbf{x}) - \underbrace{V_l(\mathbf{x}) D_l(\mathbf{x}) W_l^\top}_{V_{l-1}^\top(\mathbf{x})} \mathbf{f}_{l-1}(\mathbf{x}) \right] \quad (18)$$

$$= D_{l-1}(\mathbf{x}) V_{l-1}^\top(\mathbf{x}) [V_{l-1}^*(\mathbf{x}) \mathbf{f}_{l-1}^*(\mathbf{x}) - V_{l-1}(\mathbf{x}) \mathbf{f}_{l-1}(\mathbf{x})] \quad (19)$$

$$= D_{l-1}(\mathbf{x}) [A_{l-1}(\mathbf{x}) \mathbf{f}_{l-1}^*(\mathbf{x}) - B_{l-1}(\mathbf{x}) \mathbf{f}_{l-1}(\mathbf{x})] \quad (20)$$

□

9.2 THEOREM 1

Proof. By definition of SGD critical point, we know that for any batch \mathcal{B}_j , Eqn. 1 vanishes:

$$\dot{W}_l = \mathbb{E}_{\mathbf{x}} [\mathbf{g}_l(\mathbf{x}; \hat{\mathcal{W}}) \mathbf{f}_{l-1}^\top(\mathbf{x}; \hat{\mathcal{W}})] = \sum_{i \in \mathcal{B}_j} \mathbf{g}_l(\mathbf{x}_i; \hat{\mathcal{W}}) \mathbf{f}_{l-1}^\top(\mathbf{x}_i; \hat{\mathcal{W}}) = 0 \quad (21)$$

Let $U_i = \mathbf{g}_l(\mathbf{x}_i; \hat{\mathcal{W}}) \mathbf{f}_{l-1}^\top(\mathbf{x}_i; \hat{\mathcal{W}})$. Note that \mathcal{B}_j can be any subset of samples from the data distribution. Therefore, for a dataset of size N , Eqn. 21 holds for all $\binom{N}{|\mathcal{B}_j|}$ batches, but there are only N data samples. With simple Gaussian elimination we know that for any $i_1 \neq i_2$, $U_{i_1} = U_{i_2} = U$. Plug that into Eqn. 21 we know $U = 0$ and thus for any i , $U_i = 0$. Since U_i is an outer product, the theorem follows. □

9.3 COROLLARY 1

Proof. The base case is that $V_L(\mathbf{x}) = V_L^*(\mathbf{x}) = I_{C \times C}$, which is constant (and thus piece-wise constant) over the entire input space. If for layer l , $V_l(\mathbf{x})$ and $V_l^*(\mathbf{x})$ are piece-wise constant, then by Eqn. 4 (rewrite it here):

$$V_{l-1}(\mathbf{x}) = V_l(\mathbf{x}) D_l(\mathbf{x}) W_l^\top, \quad V_{l-1}^*(\mathbf{x}) = V_l^*(\mathbf{x}) D_l^*(\mathbf{x}) W_l^{*\top} \quad (22)$$

since $D_l(\mathbf{x})$ and $D_l^*(\mathbf{x})$ are piece-wise constant and W_l^\top and $W_l^{*\top}$ are constant, we know that for layer $l-1$, $V_{l-1}(\mathbf{x})$ and $V_{l-1}^*(\mathbf{x})$ are piece-wise constant. Therefore, for all $l = 1, \dots, L$, $V_l(\mathbf{x})$ and $V_l^*(\mathbf{x})$ are piece-wise constant.

Therefore, $A_l(\mathbf{x})$ and $B_l(\mathbf{x})$ are piece-wise constant with respect to input \mathbf{x} . They separate the region R_0 into constant regions with boundary points in a zero-measured set. □

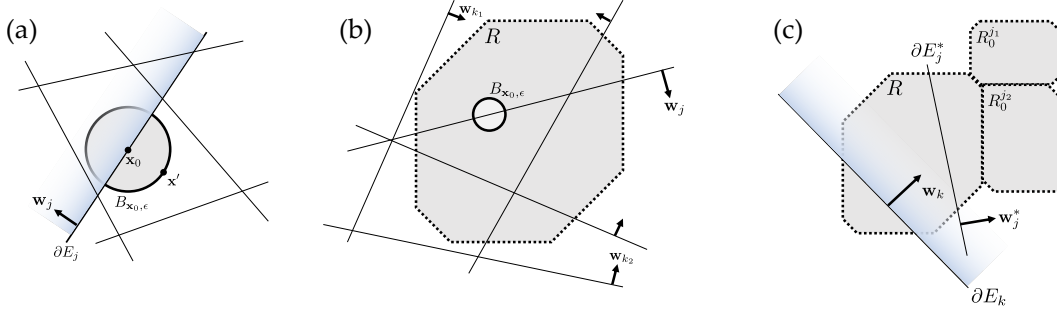


Figure 14: Proof illustration for (a) Lemma 2, (b) Lemma 3 and (c) Theorem 4.

9.4 LEMMA 2

Lemma 2. Consider K ReLU activation functions $f_j(\mathbf{x}) = \sigma(\mathbf{w}_j^\top \mathbf{x})$ for $j = 1 \dots K$. If $\mathbf{w}_j \neq 0$ and no two weights are co-linear, then $\sum_{j'} c_{j'} f_{j'}(\mathbf{x}) = 0$ for all $\mathbf{x} \in \mathbb{R}^{d+1}$ suggests that all $c_j = 0$.

Proof. Suppose there exists some $c_j \neq 0$ so that $\sum_j c_j f_j(\mathbf{x}) = 0$ for all \mathbf{x} . Pick a point $\mathbf{x}_0 \in \partial E_j$ so that $\mathbf{w}_j^\top \mathbf{x}_0 = 0$ but all $\mathbf{w}_{j'}^\top \mathbf{x}_0 \neq 0$ for $j' \neq j$, which is possible due to the distinct weight conditions. Consider an ϵ -ball $B_{\mathbf{x}_0, \epsilon} = \{\mathbf{x} : \|\mathbf{x} - \mathbf{x}_0\| \leq \epsilon\}$. We pick ϵ so that $\text{sign}(\mathbf{w}_{j'}^\top \mathbf{x})$ for all $j' \neq j$ remains the same within $B_{\mathbf{x}_0, \epsilon}$ (Fig. 14(a)). Denote $[j^+]$ as the indices of activated ReLU functions in $B_{\mathbf{x}_0, \epsilon}$ except j .

Then for all $\mathbf{x} \in B_{\mathbf{x}_0, \epsilon} \cap E_j$, we have:

$$h(\mathbf{x}) \equiv \sum_{j'} c_{j'} f_{j'}(\mathbf{x}) = c_j \mathbf{w}_j^\top \mathbf{x} + \sum_{j' \in [j^+]} c_{j'} \mathbf{w}_{j'}^\top \mathbf{x} = 0 \quad (23)$$

Since $B_{\mathbf{x}_0, \epsilon}$ is a d -dimensional object rather than a subspace, for \mathbf{x}_0 and $\mathbf{x}_0 + \epsilon \mathbf{e}_k \in B_{\mathbf{x}_0, \epsilon}$, we have

$$h(\mathbf{x}_0 + \epsilon \mathbf{e}_k) - h(\mathbf{x}_0) = \epsilon(c_j w_{jk} + \sum_{j' \in [j^+]} c_{j'} w_{j'k}) = 0 \quad (24)$$

where \mathbf{e}_k is axis-aligned unit vector ($1 \leq k \leq d$). This yields

$$c_j \tilde{\mathbf{w}}_j + \sum_{j' \in [j^+]} c_{j'} \tilde{\mathbf{w}}_{j'} = \mathbf{0}_d \quad (25)$$

Plug it back to Eqn. 23 yields

$$c_j b_j + \sum_{j' \in [j^+]} c_{j'} b_{j'} = 0 \quad (26)$$

where means that for the (augmented) $d+1$ dimensional weight:

$$c_j \mathbf{w}_j + \sum_{j' \in [j^+]} c_{j'} \mathbf{w}_{j'} = \mathbf{0}_{d+1} \quad (27)$$

However, if we pick $\mathbf{x}' = \mathbf{x}_0 - \epsilon \frac{\tilde{\mathbf{w}}_j}{\|\tilde{\mathbf{w}}_j\|^2} \in B_{\mathbf{x}_0, \epsilon} \cap E_j^c$, then $f_j(\mathbf{x}') = 0$ but $\sum_{j' \in [j^+]} f_{j'}(\mathbf{x}') = -c_j \mathbf{w}_j^\top \mathbf{x}' = \epsilon c_j$ and thus

$$\sum_{j'} c_{j'} f_{j'}(\mathbf{x}') = \epsilon c_j \neq 0 \quad (28)$$

which is a contradiction. \square

9.5 LEMMA 3

Lemma 3 (Local ReLU Independence). *Let R be an open set. Consider K ReLU nodes $f_j(\mathbf{x}) = \sigma(\mathbf{w}_j^\top \mathbf{x})$, $j = 1, \dots, K$. $\mathbf{w}_j \neq 0$, $\mathbf{w}_j \neq \gamma \mathbf{w}_{j'}$ for $j \neq j'$ with any $\gamma > 0$.*

If there exists $c_1, \dots, c_K, c_\bullet$ so that the following is true:

$$\sum_j c_j f_j(\mathbf{x}) + c_\bullet \mathbf{w}_j^\top \mathbf{x} = 0, \quad \forall \mathbf{x} \in R \quad (29)$$

and for node j , $\partial E_j \cap R \neq \emptyset$, then $c_j = 0$.

Proof. We can apply the same logic as Lemma 2 to the region R (Fig. 14(b)). For any node j , since its boundary ∂E_j is in R , we can find a similar \mathbf{x}_0 so that $\mathbf{x}_0 \in \partial E_j \cap R$ and $\mathbf{x}_0 \notin \partial E_{j'}$ for any $j' \neq j$. We construct $B_{\mathbf{x}_0, \epsilon}$. Since R is an open set, we can always find $\epsilon > 0$ so that $B_{\mathbf{x}_0, \epsilon} \subseteq R$ and no other boundary is in this ϵ -ball. Following similar logic of Lemma 2, $c_j = 0$. \square

9.6 LEMMA 4

Lemma 4 (Relation between Hyperplanes). *Let \mathbf{w}_j and $\mathbf{w}_{j'}$ two distinct hyperplanes with $\|\tilde{\mathbf{w}}_j\| = \|\tilde{\mathbf{w}}_{j'}\| = 1$. Denote $\theta_{jj'}$ as the angle between the two vectors \mathbf{w}_j and $\mathbf{w}_{j'}$. Then there exists $\tilde{\mathbf{u}}_{j'} \perp \tilde{\mathbf{w}}_j$ and $\mathbf{w}_{j'}^\top \tilde{\mathbf{u}}_{j'} = \sin \theta_{jj'}$.*

Proof. Note that the projection of $\tilde{\mathbf{w}}_{j'}$ onto $\tilde{\mathbf{w}}_j$ is:

$$\tilde{\mathbf{u}}_{j'} = \frac{1}{\sin \theta_{jj'}} P_{\tilde{\mathbf{w}}_j}^\perp \tilde{\mathbf{w}}_{j'} \quad (30)$$

It is easy to verify that $\|\tilde{\mathbf{u}}_{j'}\| = 1$ and $\mathbf{w}_{j'}^\top \tilde{\mathbf{u}}_{j'} = \sin \theta_{jj'}$. \square

9.7 LEMMA 5

Lemma 5 (Evidence of Data points on Misalignment). *Let $R \subset \mathbb{R}^d$ be an open set. Consider K ReLU nodes $f_j(\mathbf{x}) = \sigma(\mathbf{w}_j^\top \mathbf{x})$, $j = 1, \dots, K$. The weight component (without bias) has $\|\tilde{\mathbf{w}}_j\|_2 = 1$, \mathbf{w}_j are not co-linear. Then for a node j with $\partial E_j \cap R \neq \emptyset$, and $\epsilon \leq \epsilon_0$, either of the conditions holds:*

(1) *There exists node $j' \neq j$ so that $\sin \tilde{\theta}_{jj'} \leq MK\epsilon^{1-\delta}/|c_j|$ and $|b_{j'} - b_j| \leq M_2\epsilon^{1-2\delta}/|c_j|$.*

(2) *There exists $\mathbf{x}_j \in \partial E_j \cap R$ so that for any $j' \neq j$, $|\mathbf{w}_{j'}^\top \mathbf{x}_j| > 5\epsilon/|c_j|$.*

where $\tilde{\theta}_{jj'}$ is the angle between $\tilde{\mathbf{w}}_j$ and $\tilde{\mathbf{w}}_{j'}$, $\delta > 0$, r is the radius of a $d-1$ dimensional ball contained in $\partial E_j \cap R$, $M = \frac{10\epsilon_0^\delta}{r} \sqrt{\frac{d}{2\pi}}$, $M_0 = \max_{\mathbf{x} \in \partial E_j \cap R} \|\mathbf{x}\|$ and $M_2 = 2M_0MK\epsilon_0^\delta + 5\epsilon_0^{2\delta}$.

Proof. Define $q_j = 5\epsilon/|c_j|$. For each $j' \neq j$, define $I_{j'} = \{\mathbf{x} : |\mathbf{w}_{j'}^\top \mathbf{x}| \leq q_j, \mathbf{x} \in \partial E_j\}$. We prove by contradiction. Suppose for any $j' \neq j$, $\sin \tilde{\theta}_{jj'} > KM\epsilon^{1-\delta}/|c_j|$ or $|b_{j'} - b_j| > M_2\epsilon^{1-2\delta}/|c_j|$. Otherwise the theorem already holds.

Case 1. When $\sin \tilde{\theta}_{jj'} > KM\epsilon^{1-\delta}/|c_j|$ holds.

From Lemma 4, we know that for any $\mathbf{x} \in \partial E_j$, if $\mathbf{w}_{j'}^\top \mathbf{x} = -q_j$, with $a_{j'} \leq 2q_j|c_j|/MK\epsilon^{1-\delta} = 10\epsilon^\delta/MK$, we have $\mathbf{x}' = \mathbf{x} + a_{j'}\tilde{\mathbf{u}}_{j'} \in \partial E_j$ and $\mathbf{w}_{j'}^\top \mathbf{x}' = +q_j$.

Consider a $d-1$ -dimensional sphere $B \subseteq \Omega_j$ and its intersection of $I_{j'} \cap B$ for $j' \neq j$. Suppose the sphere has radius r . For each $I_{j'} \cap B$, its $d-1$ -dimensional volume is upper bounded by:

$$V(I_{j'} \cap B) \leq a_{j'} V_{d-2}(r) \leq \epsilon^\delta \frac{10}{MK} V_{d-2}(r) \quad (31)$$

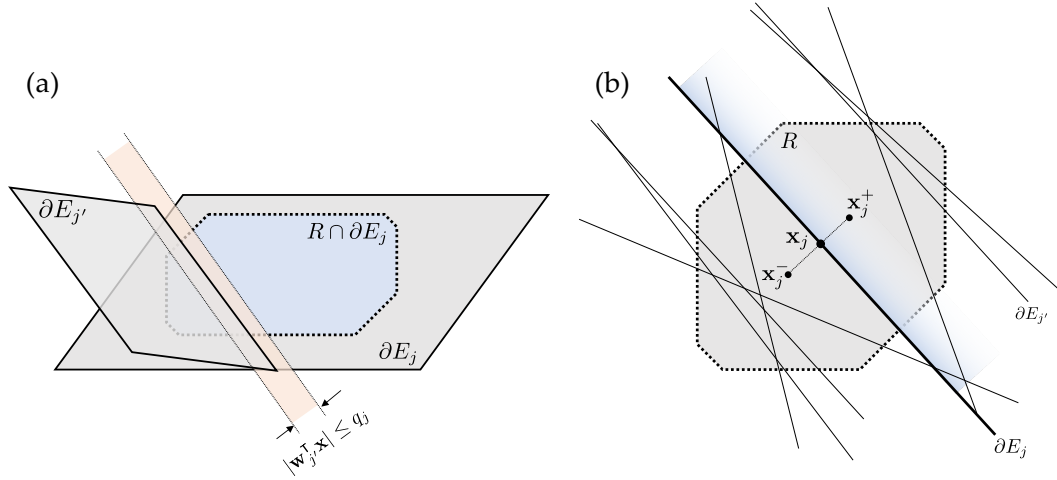


Figure 15: (a) Lemma 5. (b) Lemma 6.

where $V_{d-2}(r)$ is the $d-2$ -dimensional volume of a sphere of radius r . Intuitively, the intersection between $\mathbf{w}_{j'}^T \mathbf{x} = -q_j$ and B is at most a $d-2$ -dimensional sphere of radius r , and the “height” is at most $a_{j'}$.

Case 2. When $\sin \tilde{\theta}_{jj'} \leq KM\epsilon^{1-\delta}/|c_j|$ but $|b_{j'} - b_j| > M_2\epsilon^{1-2\delta}/|c_j|$ holds.

In this case, we want to show that for any $\mathbf{x} \in \Omega_j$, $|\mathbf{w}_{j'}^T \mathbf{x}| > q_j$ and thus $I_{j'} \cap B = \emptyset$. If this is not the case, then there exists $\mathbf{x} \in \Omega_j$ so that $|\mathbf{w}_{j'}^T \mathbf{x}| \leq q_j$. Then since $\mathbf{x} \in \partial E_j$, we have:

$$|\mathbf{w}_{j'}^T \mathbf{x}| = |(\mathbf{w}_{j'} - \mathbf{w}_j)^T \mathbf{x}| = |(\tilde{\mathbf{w}}_{j'} - \tilde{\mathbf{w}}_j)^T \tilde{\mathbf{x}} + (b_{j'} - b_j)| \leq q_j \quad (32)$$

Therefore, from Cauchy inequality and triangle inequality, we have:

$$\|\tilde{\mathbf{w}}_{j'} - \tilde{\mathbf{w}}_j\| \|\tilde{\mathbf{x}}\| \geq |(\tilde{\mathbf{w}}_{j'} - \tilde{\mathbf{w}}_j)^T \tilde{\mathbf{x}}| \geq |b_{j'} - b_j| - |\mathbf{w}_{j'}^T \mathbf{x}| \quad (33)$$

From the condition, we have $\|\tilde{\mathbf{w}}_{j'} - \tilde{\mathbf{w}}_j\| = 2 \sin \frac{\tilde{\theta}_{jj'}}{2} \leq 2 \sin \tilde{\theta}_{jj'} \leq 2KM\epsilon^{1-\delta}/|c_j|$. Then

$$2M_0MK\epsilon^{1-\delta}/|c_j| \geq |(\tilde{\mathbf{w}}_{j'} - \tilde{\mathbf{w}}_j)^T \tilde{\mathbf{x}}| \geq |b_{j'} - b_j| - q_j > M_2\epsilon^{1-2\delta}/|c_j| - 5\epsilon/|c_j| \quad (34)$$

which is equivalent to:

$$2M_0MK\epsilon^\delta > M_2 - 5\epsilon^{2\delta} \quad (35)$$

which means that

$$M_2 < 2M_0MK\epsilon^\delta + 5\epsilon^{2\delta} \leq 2M_0MK\epsilon_0^\delta + 5\epsilon_0^{2\delta} \quad (36)$$

for $\epsilon \leq \epsilon_0$. This is a contradiction. Therefore, $I_{j'} \cap B = \emptyset$ and thus $V(I_{j'} \cap B) = 0$.

Volume argument. Therefore, from the definition of M , we have $V(B) = V_{d-1}(r) \geq r \sqrt{\frac{2\pi}{d}} V_{d-2}(r) = \frac{10}{M} \epsilon_0^\delta V_{d-2}(r)$, then for $\epsilon \leq \epsilon_0$, we have:

$$V(B) = \frac{10}{M} \epsilon_0^\delta V_{d-2}(r) > \sum_{j' \neq j, j' \text{ in case 1}} V(I_{j'} \cap B) \quad (37)$$

This means that there exists $\mathbf{x}_j \in B \subseteq \Omega_j$ so that $\mathbf{x}_j \notin I_{j'} \cap B$ for any $j' \neq j$ and j' in case 1. That is,

$$|\mathbf{w}_{j'}^T \mathbf{x}_j| > q_j \quad (38)$$

On the other hand, for j' in case 2, the above condition holds for entire Ω_j , and thus hold for the chosen \mathbf{x}_j . \square

9.8 LEMMA 6

Lemma 6 (Local ReLU Independence, Noisy case). *Let R be an open set. Consider K ReLU nodes $f_j(\mathbf{x}) = \sigma(\mathbf{w}_j^\top \mathbf{x})$, $j = 1, \dots, K$. The weight component (without bias) has $\|\tilde{\mathbf{w}}_j\| = 1$, \mathbf{w}_j are not co-linear. If there exists $c_1, \dots, c_K, \mathbf{c}$, and $\epsilon \leq \epsilon_0$ so that the following is true:*

$$\left| \sum_j c_j f_j(\mathbf{x}) + \mathbf{c} \cdot \mathbf{w}^\top \mathbf{x} \right| \leq \epsilon, \quad \forall \mathbf{x} \in R \quad (39)$$

and for a node j , $\partial E_j \cap R \neq \emptyset$. Then there exists node $j' \neq j$ so that $\sin \tilde{\theta}_{jj'} \leq MK\epsilon^{1-\delta}/|c_j|$ and $|b_{j'} - b_j| \leq M_2\epsilon^{1-2\delta}/|c_j|$, where r, δ, M, M_2 are defined in Lemma 5 but with $r' = r - 5\epsilon/|c_j|$.

Proof. Let $q_j = 5\epsilon/|c_j|$ and $\Omega_j = \{\mathbf{x} : \mathbf{x} \in \partial E_j \cap R, B(\mathbf{x}, q_j) \subseteq R\}$. If situation (1) in Lemma 5 happens then the theorem holds. Otherwise, applying Lemma 5 with $R' = \{\mathbf{x} : \mathbf{x} \in R, B(\mathbf{x}, q_j) \subseteq R\}$ and there exists $\mathbf{x}_j \in \Omega_j$ so that

$$|\mathbf{w}_{j'}^\top \mathbf{x}_j| \geq q_j = 5\epsilon/|c_j| \quad (40)$$

Let two points $\mathbf{x}_j^\pm = \mathbf{x}_j \pm q_j \tilde{\mathbf{w}}_j \in R$. In the following we show that the three points \mathbf{x}_j and \mathbf{x}_j^\pm are on the same side of $\partial E_{j'}$ for any $j' \neq j$. This can be achieved by checking whether $(\mathbf{w}_{j'}^\top \mathbf{x}_j)(\mathbf{w}_{j'}^\top \mathbf{x}_j^\pm) \geq 0$ (Fig. 15):

$$(\mathbf{w}_{j'}^\top \mathbf{x}_j)(\mathbf{w}_{j'}^\top \mathbf{x}_j^\pm) = (\mathbf{w}_{j'}^\top \mathbf{x}_j) \left[\mathbf{w}_{j'}^\top (\mathbf{x}_j \pm q_j \tilde{\mathbf{w}}_j) \right] \quad (41)$$

$$= (\mathbf{w}_{j'}^\top \mathbf{x}_j)^2 \pm q_j (\mathbf{w}_{j'}^\top \mathbf{x}_j) \mathbf{w}_{j'}^\top \tilde{\mathbf{w}}_j \quad (42)$$

$$= |\mathbf{w}_{j'}^\top \mathbf{x}_j| (|\mathbf{w}_{j'}^\top \mathbf{x}_j| \pm q_j \mathbf{w}_{j'}^\top \tilde{\mathbf{w}}_j) \quad (43)$$

Since $|\mathbf{w}_{j'}^\top \tilde{\mathbf{w}}_j| \leq 1$, it is clear that $(\mathbf{w}_{j'}^\top \mathbf{x}_j)(\mathbf{w}_{j'}^\top \mathbf{x}_j^\pm) \geq 0$. Therefore the three points \mathbf{x}_j and \mathbf{x}_j^\pm are on the same side of $\partial E_{j'}$ for any $j' \neq j$.

Let $h(\mathbf{x}) = \sum_j c_j f_j(\mathbf{x}) + \mathbf{c} \cdot \mathbf{w}^\top \mathbf{x}$, then $|h(\mathbf{x})| \leq \epsilon$ for $\mathbf{x} \in R$. Since $\mathbf{x}_j^+ + \mathbf{x}_j^- = 2\mathbf{x}_j$, we know that all terms related to \mathbf{w}_\bullet and $\mathbf{w}_{j'}$ with $j \neq j'$ will cancel out (they are in the same side of the boundary $\partial E_{j'}$) and thus:

$$4\epsilon \geq |h(\mathbf{x}_j^+) + h(\mathbf{x}_j^-) - 2h(\mathbf{x}_j)| = |c_j q_j \mathbf{w}_j^\top \tilde{\mathbf{w}}_j| = |c_j| q_j = 5\epsilon \quad (44)$$

which is a contradiction. \square

9.9 THEOREM 2

Proof. In this situation, because $D_2(\mathbf{x}) = D_2^*(\mathbf{x}) = I$, according to Eqn. 4, $V_1(\mathbf{x}) = W_1^\top$ and $V_1^*(\mathbf{x}) = W_1^{*\top}$ are independent of input \mathbf{x} . Therefore, both A_1 and B_1 are independent of input \mathbf{x} .

From Assumption 1, since $\rho(\mathbf{x}) > 0$ in R_0 , from Theorem. 1 we know that the SGD critical points gives $\mathbf{g}_1(\mathbf{x}) = D_1(\mathbf{x}) [A_1 \mathbf{f}_1^*(\mathbf{x}) - B_1 \mathbf{f}_1(\mathbf{x})] = \mathbf{0}$. Picking node k , the following holds for every node k and every $\mathbf{x} \in R_0 \cap E_k$:

$$\alpha_k^\top \mathbf{f}^*(\mathbf{x}) - \beta_k^\top \mathbf{f}(\mathbf{x}) = \mathbf{0} \quad (45)$$

Here α_k^\top is the k -th row of A_1 , $A_1 = [\alpha_1, \dots, \alpha_{n_1}]^\top$ and similarly for β_k^\top . Note here layer index $l = 1$ is omitted for brevity.

For teacher j , suppose it is observed by student k , i.e., $\partial E_j^* \cap E_k \neq \emptyset$. Given all teacher and student nodes, note that co-linearity is a equivalent relation, we could partition these nodes into disjoint groups. Suppose node j is in group s . In Eqn. 45, if we combine all coefficients in group s together into one term $c_s \mathbf{w}_j^*$ (with $\|\mathbf{w}_j^*\| = 1$), we have:

$$c_s = \alpha_{kj} - \sum_{k' \in \text{co-linear}(j)} \|\mathbf{w}_{k'}\| \beta_{kk'} \quad (46)$$

“At most” because from Assumption 1, all teacher weights are not co-linear. Note that $\text{co-linear}(j)$ might be an empty set.

By Assumption 1, $\partial E_j^* \cap R_0 \neq \emptyset$ and by observation property, $\partial E_j^* \cap E_k \neq \emptyset$, we know that for $R = R_0 \cap E_k$, $\partial E_j^* \cap R \neq \emptyset$. Applying Lemma 3, we know that $c_s = 0$. Since $\alpha_{kj} \neq 0$, we know $\text{co-linear}(j) \neq \emptyset$ and there exists at least one student k' that is aligned with the teacher j . \square

9.10 THEOREM 3

Proof. We basically apply the same logic as in Theorem 2. Consider the colinear group $\text{co-linear}(k)$. If for all $k' \in \text{co-linear}(k)$, $\beta_{k_o, k'} \equiv \|\mathbf{v}_{k'}\|^2 = 0$, then $\mathbf{v}_{k'} = \mathbf{0}$ and the proof is complete.

Otherwise, if there exists some student k so that $\mathbf{v}_k \neq \mathbf{0}$. By the condition, it is observed by some student node k_o , then with the same logic we will have

$$\sum_{k' \in \text{co-linear}(k)} \beta_{k_o, k'} \|\mathbf{w}_{k'}\| = 0 \quad (47)$$

which is

$$\mathbf{v}_{k_o}^\top \sum_{k' \in \text{co-linear}(k)} \mathbf{v}_{k'} \|\mathbf{w}_{k'}\| = 0 \quad (48)$$

Since k is observed by C students $k_o^1, k_o^2, \dots, k_o^J$, then we have:

$$\mathbf{v}_{k_o^j}^\top \sum_{k' \in \text{co-linear}(k)} \mathbf{v}_{k'} \|\mathbf{w}_{k'}\| = 0 \quad (49)$$

By the condition, all the C vectors $\mathbf{v}_{k_o^j}^\top \in \mathbb{R}^C$ are linear independent, then we know that

$$\sum_{k' \in \text{co-linear}(k)} \mathbf{v}_{k'} \|\mathbf{w}_{k'}\| = \mathbf{0} \quad (50)$$

□

9.11 COROLLARY 2

Proof. We can write the contribution of all student nodes which are not aligned with any teacher nodes as follows:

$$\sum_s \sum_{k \in \text{co-linear}(s)} \mathbf{v}_k f_k(\mathbf{x}) = \sum_s \sum_{k \in \text{co-linear}(s)} \mathbf{v}_k \|\mathbf{w}_k\| \sigma(\mathbf{w}_s'^\top \mathbf{x}) \quad (51)$$

$$= \sum_s \sigma(\mathbf{w}_s'^\top \mathbf{x}) \sum_{k \in \text{co-linear}(s)} \mathbf{v}_k \|\mathbf{w}_k\| \quad (52)$$

where \mathbf{w}_s' is the unit vector that represents the common direction of the co-linear group s . From Theorem 3, for group s that is not aligned with any teacher, $\sum_{k \in \text{co-linear}(s)} \mathbf{v}_k \|\mathbf{w}_k\| = \mathbf{0}$ and thus the net contribution is zero. □

9.12 THEOREM 4

Proof. In multi-layer case, $A_l(\mathbf{x})$ and $B_l(\mathbf{x})$ are no longer constant over input \mathbf{x} . Fortunately, thanks to the recursive definition (Eqn. 4) which only contains input-independent terms (weights) and gating function, $A_l(\mathbf{x})$ and $B_l(\mathbf{x})$ are piece-wise constant function over the input R_0 .

Note that R_0 can be partitioned into $\mathcal{R} = \{R_0^1, R_0^2, \dots, R_0^J\}$ and a zero-measure set. Each of them is constant region for $A_l(\mathbf{x})$ and $B_l(\mathbf{x})$. Since R_0^j is an intersection of finite open half-planes (from k 's parent nodes), R_0^j is still an open set.

From the condition, there exists open set $R \in \mathcal{R}$ and a student observer node k so that $\partial E_j^* \cap E_k \cap R \neq \emptyset$ (Fig. 14(c)). Let H_R and similarly H_R^* be the student and teacher nodes whose boundary intersects with R . Therefore $j \in H_R^*$. For other teacher/student nodes, they are linear functions within R and thus can be combined together into $\mathbf{w}_*^\top \mathbf{x}$. For all weights in H_R, H_R^* and \mathbf{w}_* , applying Lemma 3 on $R \cap E_k$, we know that the SGD critical point $\alpha_{R,k}^\top \mathbf{f}_1^*(\mathbf{x}) - \beta_{R,k}^\top \mathbf{f}_1(\mathbf{x}) = \mathbf{0}$ leads to alignment between H_R and H_R^* . Let group s be the one that contains all weights that are co-linear to teacher node j (note that no other teacher nodes are involved), and c_s its coefficient. Since $j \in H_R^*$, $c_s = 0$. Since $\alpha_{kj}(R) \neq 0$, there exists at least one student node k' that is co-linear to teacher node j .

□

9.13 THEOREM 5

Proof. We follow the logic of Theorem 4. Instead of applying Lemma 3, for gradient that is not zero but bounded within ϵ , we pick the student observer k and we have for $E_k \cap R$:

$$|\alpha_k^\top \mathbf{f}^*(\mathbf{x}) - \beta_k^\top \mathbf{f}(\mathbf{x})| \leq \epsilon, \quad (53)$$

we use Lemma 6 and know that there exists a node $k' \neq j$ so that $\sin \tilde{\theta}_{k'j} = \mathcal{O}(\epsilon^{1-\delta}/|c_j|)$ and $|b_{k'} - b_j^*| = \mathcal{O}(\epsilon^{1-2\delta}/|c_j|)$ for any $\delta > 0$. Under the observation of student k , the teacher j has coefficient $c_j = \alpha_{kj} \|\tilde{\mathbf{w}}_j^*\|$ (since the teacher need to be re-normalized for Lemma 6 to be applicable). Since all teacher weights are distant to each other with positive constant $b_0 > 0$ and $\theta_0 > 0$, with sufficiently small ϵ_0 and $\epsilon \leq \epsilon_0$, this node k' has to be a student node and the bound follows. \square

9.14 THEOREM 6

Proof. From the expression we can see that it is positive homogeneous with respect to $\|\mathbf{w}_j^*\|$ and $\|\mathbf{w}_k\|$. So we can assume $\|\mathbf{w}_j^*\| = \|\mathbf{w}_k\| = 1$. Without loss of generality, we set up the coordinate system so that $\mathbf{w}_j^* = [1, 0]^\top$ and $\mathbf{w}_k = [\cos \theta, \sin \theta]^\top$. Then

$$\mathbb{E}_{\mathbf{x}} [\mathbf{f}_{l-1} z_k f_j^*] = \mathbb{E}_{\mathbf{x}} [\mathbf{f}_{l-1} z_k z_j^* \mathbf{f}_{l-1}^\top] \mathbf{w}_j^* = \sum_{\mathbf{f}_{l-1}^\top \mathbf{w}_j^* \geq 0, \mathbf{f}_{l-1}^\top \mathbf{w}_k \geq 0} \mathbf{f}_{l-1} \mathbf{f}_{l-1}^\top \mathbf{w}_j^* \quad (54)$$

$$= \int_0^{+\infty} r^2 p(r) \int_{-\frac{\pi}{2}+\theta}^{\frac{\pi}{2}} \begin{bmatrix} \cos \theta' \\ \sin \theta' \end{bmatrix} \cos \theta' p(\theta'|r) d\theta' + \epsilon \quad (55)$$

where ϵ is the term reflecting the asymmetry of the data distribution $p(\mathbf{f}_{l-1})$ with respect to the plane spanned by the vectors \mathbf{w}_k and \mathbf{w}_j^* .

If the data distribution $p(\mathbf{f}_{l-1})$ is scale invariant (rescaling the data point won't change the angular distribution), then $p(\theta'|r) = p(\theta')$ and we only need to check the angular integral:

$$\mathbf{I}(\theta) = \int_{-\frac{\pi}{2}+\theta}^{\frac{\pi}{2}} \begin{bmatrix} \cos \theta' \\ \sin \theta' \end{bmatrix} \cos \theta' p(\theta') d\theta' \quad (56)$$

Note that $\cos^2 \theta = \frac{1}{2}(1 + \cos 2\theta)$ and $\sin \theta \cos \theta = \frac{1}{2} \sin 2\theta$, so we have:

$$2\mathbf{I}(\theta) = \left(\int_{-\frac{\pi}{2}+\theta}^{\frac{\pi}{2}} p(\theta') d\theta' \right) \mathbf{w}_j^* + \int_{-\frac{\pi}{2}+\theta}^{\frac{\pi}{2}} \begin{bmatrix} \cos 2\theta' \\ \sin 2\theta' \end{bmatrix} p(\theta') d\theta' \quad (57)$$

$$= \left(\int_{-\frac{\pi}{2}+\theta}^{\frac{\pi}{2}} p(\theta') d\theta' \right) \mathbf{w}_j^* + \frac{1}{2} \int_{2\theta}^{2\pi} \begin{bmatrix} \cos \theta'' \\ \sin \theta'' \end{bmatrix} p\left(\frac{\theta''}{2} - \frac{\pi}{2}\right) d\theta'' \quad (58)$$

$$= I_1(\theta) \mathbf{w}_j^* + \frac{1}{2} \mathbf{I}_0 - \frac{1}{2} \mathbf{I}_2(\theta) \quad (59)$$

where $\theta'' = 2\theta' + \pi$ and

$$I_1(\theta) = \int_{-\frac{\pi}{2}+\theta}^{\frac{\pi}{2}} p(\theta') d\theta' \quad (60)$$

$$\mathbf{I}_0 = \int_0^{2\pi} \begin{bmatrix} \cos \theta'' \\ \sin \theta'' \end{bmatrix} p\left(\frac{\theta''}{2} - \frac{\pi}{2}\right) d\theta'' \quad (61)$$

$$\begin{aligned} \mathbf{I}_2(\theta) &= \int_0^{2\theta} \begin{bmatrix} \cos \theta'' \\ \sin \theta'' \end{bmatrix} p\left(\frac{\theta''}{2} - \frac{\pi}{2}\right) d\theta'' \\ &= \left\{ \int_0^\theta \left[p\left(\frac{\theta'}{2} - \frac{\pi}{2}\right) + p\left(\theta - \frac{\theta'}{2} - \frac{\pi}{2}\right) \right] \cos \theta' d\theta' \right\} \mathbf{w}_k \\ &\quad + \left\{ \int_0^\theta \left[p\left(\frac{\theta'}{2} - \frac{\pi}{2}\right) - p\left(\theta - \frac{\theta'}{2} - \frac{\pi}{2}\right) \right] \sin \theta' d\theta' \right\} \mathbf{w}_k^\perp \end{aligned} \quad (62)$$

where \mathbf{w}_k^\perp is the unit vector that is perpendicular to \mathbf{w}_k but still in the plane spanned by \mathbf{w}_k and \mathbf{w}_j^* . Note \mathbf{I}_0 is the fixed integral of unit vectors weighted by angular distribution of input data on activated half-plane E_j^* of teacher node j .

If $p(\mathbf{f}_{l-1})$ is rotational symmetric, then $\epsilon = \mathbf{0}$, $p(\theta') = \frac{1}{2\pi}$, then we can compute these terms analytically: $\mathbf{I}_0 = \mathbf{0}$, $I_1(\theta) = \frac{1}{2\pi}(\pi - \theta)$ and $\mathbf{I}_2(\theta) = \frac{1}{\pi} \sin \theta \mathbf{w}_k$. \square

9.15 THEOREM 7

Proof. Note that we have:

$$\frac{d}{dt} \|\mathbf{w}_k\| = \frac{d}{dt} \sqrt{\|\mathbf{w}_k\|^2} = \frac{2\mathbf{w}_k^\top \dot{\mathbf{w}}_k}{2\|\mathbf{w}_k\|} = \frac{1}{\|\mathbf{w}_k\|} \mathbf{w}_k^\top \dot{\mathbf{w}}_k = \mathbf{w}_k^\top \mathbf{r}_k \quad (63)$$

Therefore, we have

$$\frac{d}{dt} \ln \|\mathbf{w}_k\| = \bar{\mathbf{w}}_k^\top \mathbf{r}_k \quad (64)$$

and

$$\frac{d}{dt} \left(\ln \frac{\|\mathbf{w}_k\|}{\|\mathbf{w}_{k'}\|} \right) = \frac{d}{dt} (\ln \|\mathbf{w}_k\| - \ln \|\mathbf{w}_{k'}\|) = \bar{\mathbf{w}}_k^\top \mathbf{r}_k - \bar{\mathbf{w}}_{k'}^\top \mathbf{r}_{k'} \quad (65)$$

Note that we have:

$$\frac{d}{dt} \bar{\mathbf{w}}_k = \frac{d}{dt} \left(\frac{\mathbf{w}_k}{\|\mathbf{w}_k\|} \right) = \mathbf{r}_k - \mathbf{w}_k \frac{\mathbf{w}_k^\top \mathbf{r}_k}{\|\mathbf{w}_k\|^2} = (I - \bar{\mathbf{w}}_k \bar{\mathbf{w}}_k^\top) \mathbf{r}_k = P_{\bar{\mathbf{w}}_k}^\perp \mathbf{r}_k \quad (66)$$

Let $h_k = \bar{\mathbf{w}}_k^\top \mathbf{r}_k$. We assume all $h_k > 0$ (positive correlation), then we have:

$$\frac{d}{dt} h_k = \mathbf{r}_k^\top P_{\bar{\mathbf{w}}_k}^\perp \mathbf{r}_k + \bar{\mathbf{w}}_k^\top \dot{\mathbf{r}}_k = \|\mathbf{r}_k\|^2 - h_k^2 + \bar{\mathbf{w}}_k^\top \dot{\mathbf{r}}_k \quad (67)$$

If $\mathbf{r}_k = \mathbf{r} = \mathbf{w}^* - \sum_k a_k \mathbf{w}_k$, then we have:

$$\frac{d}{dt} h_k = \|\mathbf{r}\|^2 - h_k^2 - S h_k \quad (68)$$

where $S = (\sum_k a_k \|\mathbf{w}_k\|) > 0$ is independent of k . So

$$\frac{d}{dt} (h_k - h_{k'}) = (h_{k'}^2 - h_k^2) + S(h_{k'} - h_k) = (h_{k'} - h_k)(h_{k'} + h_k + S) \quad (69)$$

if $h_k - h_{k'} > 0$, then $\frac{d}{dt} (h_k - h_{k'}) < 0$ and vice versa. This means that Eqn. 65 is zero when the system enters the stable region. On the other hand, if $\|\mathbf{r}_k\|^2 = \|\mathbf{r}_{k'}\|^2 + \epsilon$ (e.g., \mathbf{r}_k has stronger teacher component), then we have:

$$\frac{d}{dt} (h_k - h_{k'}) = (h_{k'} - h_k)(h_{k'} + h_k + S) + \epsilon \quad (70)$$

which is only zero when $h_k > h_{k'}$. This yields exponential growth of $\|\mathbf{w}_k\|$ compared to $\|\mathbf{w}_{k'}\|$. \square